DOKUZ EYLUL UNIVERSITY

GRADUATE SCHOOL OF NATURAL AND APPLIED SCIENCES

SYNTHESIS, CHARACTERIZATION AND APPLICATION OF SELF-HEALING COATINGS ON SEVERAL SUBSTRATES BY SPRAY TECHNIQUE

by

Merve DİLAVER

April, 2017

İZMİR

SYNTHESIS, CHARACTERIZATION AND APPLICATION OF SELF-HEALING COATINGS ON SEVERAL SUBSTRATES BY SPRAY TECHNIQUE

A Thesis Submitted to the
Graduate School of Natural and Applied Sciences of Dokuz Eylül University
In Partial Fulfillment of the Requirements for the Degree of Doctor of Philosophy in Chemistry Program

by

Merve DİLAVER

April, 2017

İZMİR

Ph.D. THESIS EXAMINATION RESULT FORM

We have read the thesis entitled **"SYNTHESIS, CHARACTERIZATION AND APPLICATION OF SELF-HEALING COATINGS ON SEVERAL SUBSTRATES BY SPRAY TECHNIQUE"** completed by **MERVE DİLAVER** under supervision of **Prof. Dr. MEHMET KADİR YURDAKOÇ** and we certify that in our opinion it is fully adequate, in scope and in quality, as a thesis for the degree of Doctor of Philosophy.

Prof. Dr. Mehmet Kadir YURDAKOÇ

Supervisor

Prof. Dr. Mustafa Yavuz ERGÜN

Thesis Committee Member

Assist. Prof. Dr. Aylin ZİYLAN

Thesis Committee Member

Prof. Dr. Mustafa M. DEMİR

Examining Committee Member

Prof. Dr. Nuraddin Golak

Examining Committee Member

Prof.Dr. Emine İlknur ÇÖCEN

Director

Graduate School of Natural and Applied Sciences

ACKNOWLEDGMENTS

The author is grateful to supervisor of this thesis, Prof. Dr. Mehmet Kadir YURDAKOÇ, for his valuable guide, help and advice, at all stages of this thesis study.

Also, I would like to thank to Prof. Dr. Mustafa Yavuz ERGÜN for his suggestions and useful comments during the preparation of the thesis.

In addition, the author wishes to express her gratefulness to all friends for their continuous helpful encouragement and valuable supports.

I am grateful to the Research Foundation of Dokuz Eylul University as Project No. 2012.KB.FEN.045 for the support and would like to thank Prof. Dr. Erdal ÇELİK and Dr. Aylin Altınışık TAĞAÇ for their valuable comments and also to Teknobim Nanotechnology Research and Development Company for the financial supports. I am also grateful to Dr. Cevher Gündoğdu HIZLIATEŞ for her contribution to the second part of the Thesis.

Finally, I would like to thank my family for bringing me in this situation with their unique patience and supports.

Merve DİLAVER

SYNTHESIS, CHARACTERIZATION AND APPLICATION OF SELF-HEALING COATINGS ON SEVERAL SUBSTRATES BY SPRAY TECHNIQUE

ABSTRACT

The self-healing concept for an epoxy polymer was investigated. This thesis composed of two different mechanistical approachs of self-healing and two experimental parts. First part is related with capsule based self healing where Melamine-formaldehyde prepolymer (MF) was used as microcapsules' shell. Dicyclopentadiene (DCPD) and Grubbs' catalyst were chosen as healing agent and catalyst, respectively. The second part deals with intrinsic self-healing based on the Diels-Alder (DA) and retro-Diels-Alder (rDA) reactions.

In case of the capsule technique, microcapsules were synthesized by polymerization of melamine and formaldehyde to form shell over DCPD droplets. Characterization of these capsules was studied by Fourier-transform infrared spectroscopy (FTIR) and Scanning Electron Microscopy (SEM) Analysis to investigate the chemical structure and surface morphology, respectively.

In the second part, thermally activated self-healing system based on the DA reaction of modified chitosan functionalized furan-maleimide carbazole polymers were studied.

In order to observe the healing effect of polymer matrix in both of two systems, Optical Microscope (OM) was used. Thermal stabilities of the prepared coatings were also investigated by TG-DTA and DSC analysis. As a conclusion, the healing efficiency reached to 89 percent after waiting in oven for 1.5h at 40 centigrade degree for the first part of the study. On the other hand, the self-healing efficiency was determined as 45.5 percent for DA-rDA type self-healing system.

Keywords: Self-healing, melamine-formaldehyde resin, dicyclopentadiene, microencapsulation, ROMP, modified chitosan, bismaleimide, Diels-Alder reaction

KENDİ KENDİNE İYİLEŞEN KAPLAMALARIN SENTEZİ, KARAKTERİZASYONU VE SPREY TEKNİĞİ İLE FARKLI SUBSTRATLAR ÜZERİNE UYGULAMASI

ÖZ

Çalışmada self-healing kavramı epoksi polimer üzerinde incelenmiştir. Tez, iki farklı kendi kendini onarma mekanizma yaklaşımı ve iki denel kısımdan oluşmaktadır. Birinci kısım, Melamin-formaldehit (MF) önpolimerinin mikrokapsül kabuğu olarak kullanıldığı kapsüle dayalı kendi kendini onarmayla ilgilidir. İkinci kısım, Diels-Alder (DA) ve retro-Diels-Alder (rDA) tepkimelerinin kullanıldığı içsel kendi kendini onarmayla ilgilidir.

Kapsül tekniğinde, Disiklopentadien (DCPD) ve Grubbs' katalizörü sırasıyla iyileştirme ajanı ve katalizör olarak seçilmiştir. Mikrokapsüller, melamin ve formaldehitin polimerleşerek Disiklopentadien damlalarının çevresi sarması ile oluşturulur. Mikrokapsüllerin karakterizasyonu, Fourier-transform infrared spektroskopisi (FTIR) ve Scanning Electron Mikroskopisi (SEM) sırasıyla kimyasal yapı ve yüzey morfolojisini aydınlatmak amacı ile kullanılmıştır.

İkinci kısımda, modifiye edilmiş furan fonksiyonlu maleimit karbazol polimerler arasında termal olarak aktiflenen kendi kendini onarmaya dayalı DA reaksiyonları çalışılmıştır.

Her iki sistemde polimer matriksin onarım etkisini gözlemek için Optik Mikroskop (OM) kullanılmıştır. Hazırlanan kaplamaların termal kararlılıkları da TG/DTA ve DSC analizleriyle incelenmiştir. Sonuç olarak, çalışmanın birinci kısmında 1,5 saat ve 40 santigrat derecede yüzde 89'luk bir kendi kendini onarma verimi elde edilirken, DA-rDA tepkimesine dayalı sistemde yüzde 45'lik onarım verimine ulaşılmıştır.

Anahtar kelimeler: Kendi kendine iyileştirme, melamin-formaldehit reçine, disiklopentadien, mikrokapsülleme, ROMP, modifiye kitosan, bismaleimit, Diels-Alder tepkimesi

CONTENTS

Page

LIST OF FIGURES

Page

LIST OF TABLES

Page

CHAPTER ONE
INTRODUCTION

1.1 Self-Healing

Exposing polymeric materials to harsh environmental conditions causes various deterioration in the construction of these materials. In addition, small scratches, and cracks can occur in the materials due to usage. In other words, micro-scratches and cracks may progress over time, resulting in a partial deterioration of the material or an expiration of the service life of the material. In addition, as damage progresses to the interior of the material, it also makes it difficult to repair it, the materials had better to have the ability of self-healing. In fact, it is also known that self-repair mechanisms work in nature, and there are many articles on this field (Trask, Williams & Bond, 2007; Albert & Wong, 1981).

Self-healing materials have the ability to repair and replace themselves using existing facilities. Whether the repair process is autonomic or externally assisted (e.g., by heating, to exposure UV light), the healing process begins with damage to the material. Self-healing materials offer new ways to prepare and improve our safer, longer-lasting products (Blaiszik et al., 2010).

We live in an era where important developments and progresses in different fields and disciplines, especially in science and technology. This unifying approach enables researchers to collaborate on the creation of unique creative materials by sampling organic and physical chemistry, material science and biochemistry, and electrical and mechanical engineering knowledge, exemplified in polymer science. One example of such type of material that has been undergoing tremendous growth and development in recently is known as Smart Materials (Murphy & Wuld, 2009).

These materials have healing properties. The healing process is in function either intrinsically via reversible bonds present in the material itself, or extrinsically via a pre-added healing agent which are responsing to some external stimulus. This field

covers stimuli-responsive healable materials and known beginning in the early 1990s. The research on this area is now remarkably incresing (Murphy & Wuld, 2009).

1.2 Approaches to Self-Healing

Self-healing materials can be classified into three groups: capsule based, vascular, and intrinsic. as shown in Figure 1.1. Each approach differs from the currently valid mechanism up to the damage-induced recovery process. The type of healing mechanism is determined by the volume of damage that can be cured, the reproducibility of recovery, and the recovery rate for each approach. These mechanisms are fundamental and can be presented schematically in Figure 1.1 (Blaiszik et al., 2010).

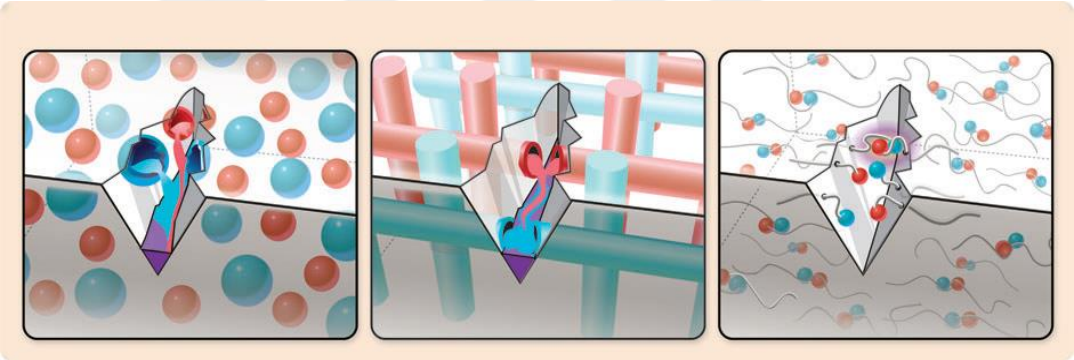

Figure 1.1 Approaches to self-healing include (Blaiszik et al., 2010).

1.2.1 Capsule-Based Self-Healing Materials

In self-healing, healing agent is placed in microcapsules. When the capsules are ruptured by damage, the self-healing mechanism is triggered through the release and reaction of the healing agent in the damage or crack medium. After release, the local healing agent is depleted, leading to only a singular local healing event (Blaiszik et al., 2010).

Capsule-based self-healing materials have been developed for some of the most commonly used synthetic polymers and elastomers. There are variety of capsule

based healing schemes. Each scheme is composed of a healing agent in a discrete capsule until damage triggers release (Blaiszik et al., 2010).

In Figure 1.2, four schemes for release of the healing agent was defined. In the first scheme (capsule-catalyst), the healing agent is an encapsulated liquid, and the polymerizer is a dispersed catalyst phase. An example of well-known capsule-catalyst system is the dicyclopentadiene (DCPD)-Grubbs' first-generation catalyst system (White et al., 2001). This system works on the basis of the ring-opening metathesis polymerization (ROMP) of DCPD via the Grubbs' catalyst. There were series of papers describing autonomic self-healing using a UF-encapsulated DCPD healing agent and Grubbs' catalyst and reported with high healing efficiencies (Brown, Sottos & White, 2002).

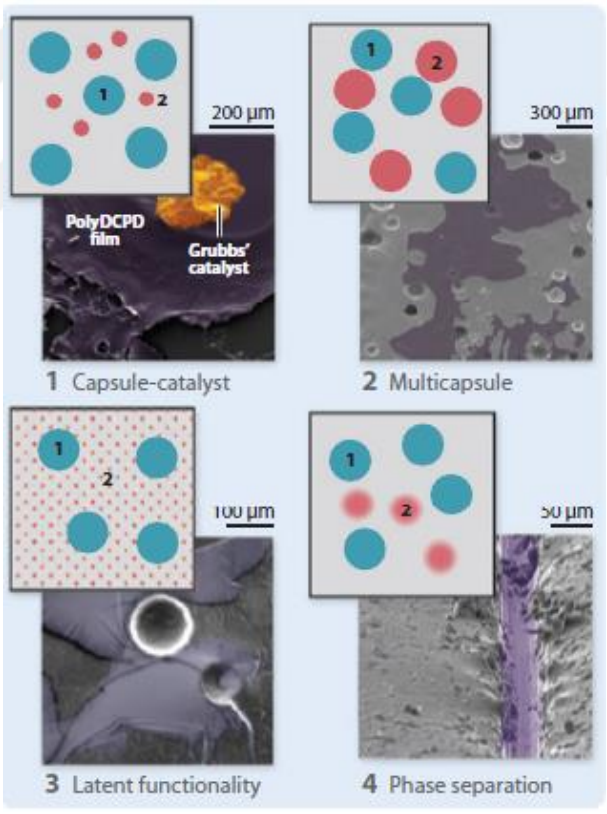

Figure 1.2 Capsule-based self-healing materials (Blaiszik et al., 2010).

In the second scheme (multicapsule), both the healing agent and the polymerizer were encapsulated. This was known as multicapsule technique which can be

expanded to include as many distinct capsule types. They were necessary to separate the reactive components of the healing system. Keller, White, & Sottos (2007); Keller, White, Sottos (2008) demonstrated multicapsule self-healing in an elastomeric matrix using two distinct capsule types composed of polydimethylsiloxane (PDMS). In this system, the healing reaction was a platinum-catalyzed hydrosilylation of vinyl-terminated PDMS resin (Keller, White, & Sottos, 2007). Furthermore, Cho, White, & Braun (2009) extended the PDMS multicapsule healing for corrosion inhibition purposes by incorporating PDMS resin capsules and dimethyldineodecanoate tin (DMDNT) catalyst capsules in an epoxy coating.

In the third scheme, the healing agent is encapsulated or dispersed as particles, and the polymerizer is residual reactive functionality in the matrix or an environmental stimulus. Kumar, Stephenson, & Murray (2006) incorporated various healing agents in PU, acrylic, and other paints. This was used for reducing the corrosion of a steel substrate.

In the fourth capsule-based scheme for self-healing, either the healing agent or the polymerizer is phase-separated in the polymeric matrix. Cho, Anderson, White, Sottos,& Braun (2006) demonstrated this concept by phase-separating hydroxyl end-functionalized polydimethylsiloxane (HOPDMS) and polydiethoxysiloxane (PDES) in epoxy vinyl ester matrix. This was used to restor the mechanical integrity and also to prevent corrosion (Cho, White, & Braun, 2009). In these systems, the tin catalysts (DBTL/DMDNT) were encapsulated for protection until matrix damage triggered their release and catalyzed the reaction with the phase-separated HOPDMS/PDES.

The original self-healing system developed by White et al. (2001) contained microencapsulated dicyclopentadiene (DCPD) monomer and a solid phase Grubbs' catalyst embedded in an epoxy matrix as shown at Figure 1.3. Damage served as the triggering mechanism when an approaching crack ruptured the embedded microcapsules releasing the DCPD into the crack plane. Ring-opening metathesis polymerization (ROMP) of the DCPD was initiated by contact with the embedded catalyst, bonding the two crack faces together. Reaction scheme was also given in

Figure 1.4. The efficiency of crack healing was calculated from the mechanical analysis (White et al., 2001). Healing efficiencies of over 90% were reported for optimized concentrations of microcapsules and catalyst (Brown, Sottos, & White, 2002). In addition to providing an efficient mechanism for self-healing, the presence of DCPD-filled microcapsules which are shown at Figure 1.5 (Brown, White, & Sottos, 2004). In this work, urea-formaldehyde (UF) microcapsules were prepared by in situ polymerization in an oil-in-water emulsion.

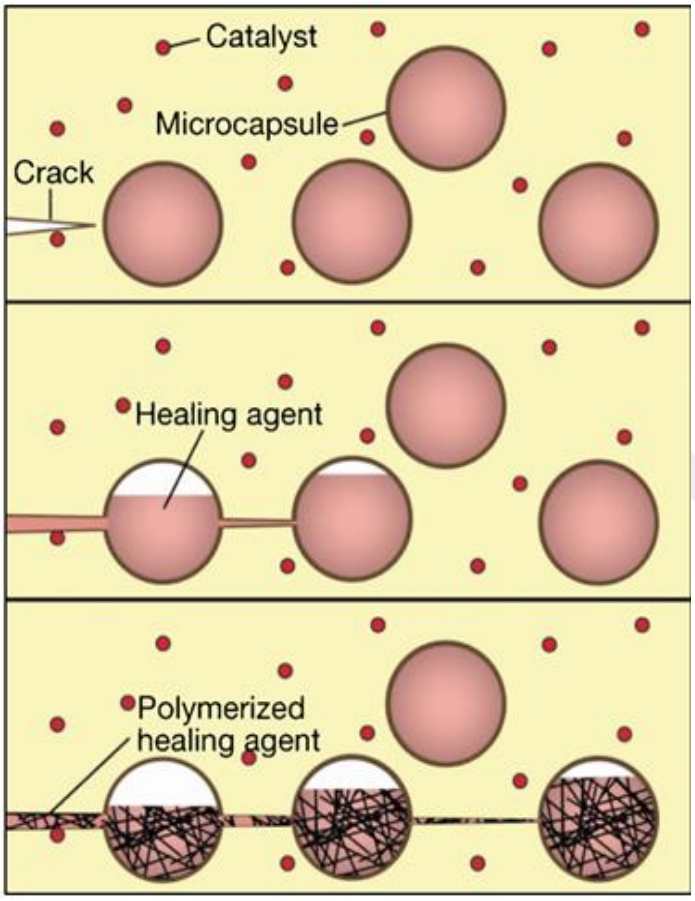

Figure 1.3 The self-healing concept where a microcapsulated healing agent is embedded in a structural composite matrix containing a catalys capable of polymerization the healing agent (White et al., 2001)

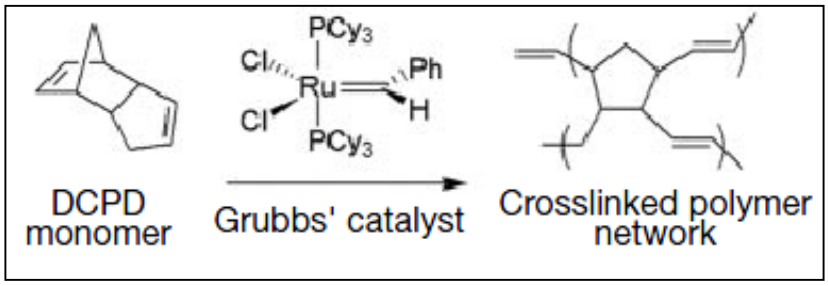

Figure 1.4 Ruthenium-based Grubbs' catalyst initiates ring-opening metathesis polymerization (ROMP) of dicyclopentadiene (DCPD) (White et al., 2001).

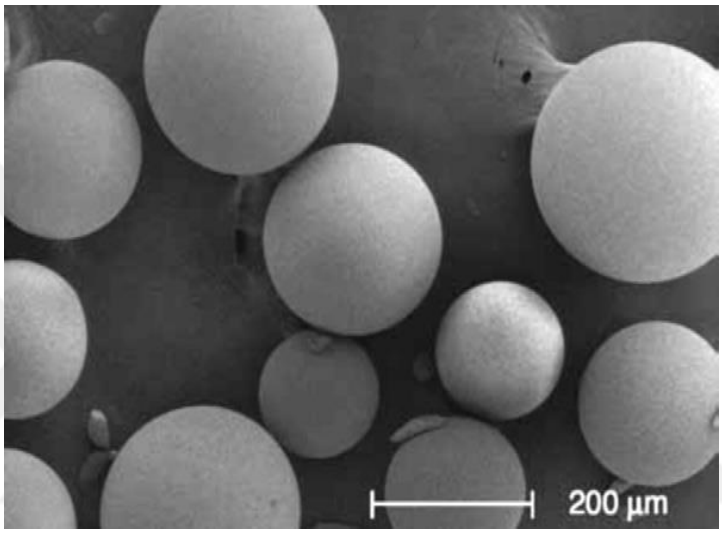

Figure 1.5 Urea-formaldehyde microcapsules containing DCPD prepared by emulsion in situ microencapsulation (Brown, White & Sottos, 2004)

A basic review of the in situ encapsulation technique has been provided by Baxter (1974), Thies (1987, 1996) and Arshady & George (1993).

In this technique, in situ encapsulation of water-immiscible liquids by the reaction of urea with formaldehyde at acid pH is outlined by Dietrich, Herma, Nastke, Bonatz, & Teige (1989). The schematic presentation of the microcapsulation was given in Figure 1.6.

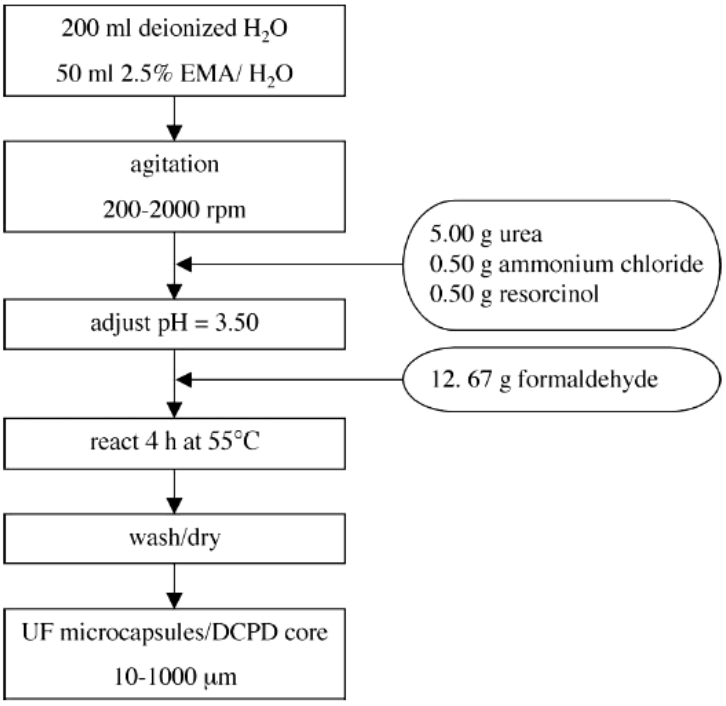

Figure 1.6 Microencapsulation of DCPD utilizing acid-catalyzed in situ polymerization of urea with formaldehyde to form capsule wall (Dietrich, Herma, Nastke, Bonatz, & Teige 1989).

In an another study, Cho, Andersson, White, Sottos, & Braun (2006) demonstrated self-healing of thermosetting epoxy vinyl esters. The Tin catalyzed polycondensation of silanol functionalized poly(dimethyl siloxane) (PDMS) was studied. In this work, a tin catalyst was encapsulated and PDMS was phase separated in the matrix. Although lower healing efficiencies were obtained compared to the DCPD and Grubbs' system. This system was resistant to deactivation by air, water, or the vinyl ester matrix. The phase separation in the healing system (Cho, Andersson, White, Sottos, & Braun, 2006) is based on the interaction of two liquid constituents to produce the healing response. This system differs from that of White et al. (2001) which was based on heterogeneous catalysis in which a fluid (the monomeric healing agent) interacts with a solid catalyst particle to initiate the healing reaction.

On the other hand, Wang et al. (2011) studied on chitosan/urea-formaldehyde shell microcapsules in which contain dicyclopentadiene. The preparation method of the microcapsules is based on electrostatic adsorption between the cationic chitosan and negatively charged sodium dodecyl sulfate (SDS) by forming a gel layer at the

interface of oil-in-water emulsion. As a result, microcapsules' shells were synthesized by the copolymerization of chitosan and UF prepolymer as shown Figure 1.7. The process and the conditions for UF prepolymer had been reported (Asua, 2002). The chitosan/urea-formaldehyde (CUF) shell microcapsules containing healing agent were also characterized by Fourier-transform infrared (FTIR) spectroscopy, scanning electronic microscope (SEM), optical microscope (OM), and thermogravimetric analyzer (TGA) to investigate their chemical structure, surface morphology, size distribution and thermal stability, respectively. The epoxy samples containing CUF microcapsules were also prepared and healing efficiency was investigated.

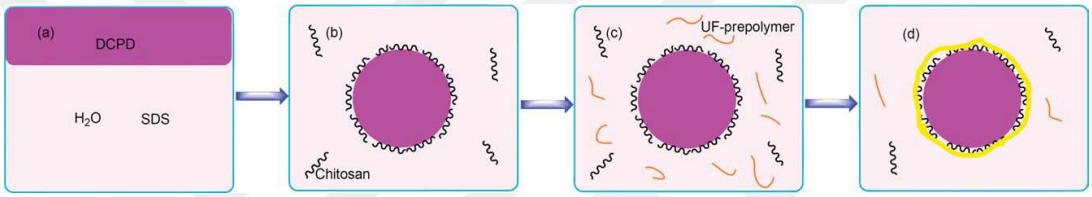

Figure 1.7 Schematic showing the formation of microcapsule (Wang et al. , 2011).

The application of microcapsules containing self-healing agents to polymeric composites is very interesting and attracted more and more attentions from researchers. The self-healing is accomplished by incorporating a microencapsulated healing agent and a catalytic chemical trigger within polymeric composites. Polymeric composites can be synthesized at different temperatures and pressures. The requirements for microcapsules containing healing agents are various according to the processing procedure of polymeric composites. The mechanical and thermal properties must be adequate to retain the intactness of microcapsules during the manufacturing of composites. The microcapsules must rupture when the damages occur. For polymeric composites processed at higher temperature and pressure, the used microcapsules must possess higher mechanical and thermal properties to resist higher temperature and pressure. The shell materials play an important role in obtaining high physical property of microcapsules. Among the various shell materials for microcapsule preparation, urea–formaldehyde (UF) resins and MF resins are widely used owing to their perfect techniques. Because PMF are superior to PUF in hardness and heat resistance (Pizzi, 1994; Dunky, 1998) the mechanical

properties and stability of PMF microcapsules may be higher than that of PUF microcapsules when they contain the same core materials.

1.2.2 Intrinsic Self-Healing Materials

Self-healing utilizing a latent material ability that is triggered by damage or an external stimulus such as heat, light, or pressure. Intrinsic self-healing materials achieve repair though inherent reversibility of bonding of the matrix polymer. Intrinsic self-healing can be accomplished through thermally reversible reactions, hydrogen bonding, ionomeric coupling, a dispersed meltable thermoplastic phase, or molecular diffusion (Blaiszik et al., 2010).

1.2.2.1 Self-healing Polymers Based on Reversible Reactions

Self-healing materials based on reversible reactions include components that can be reversibly transformed from the monomeric state to the cross-linked polymeric state by way of the addition of external energy (Bergman & Wuld, 2008). Generally, a damaged polymer is subjected to heat or intense photoillumination, triggering enhanced mobility in the damage region, bond reformation, and polymer remending (Blaiszik et al., 2010). The most widely used reaction scheme for remendable self-healing materials is based on the Diels-Alder (DA) and retro-Diels-Alder (rDA) reactions. Chen et al. (2002); Chen et al. (2003) demonstrated a thermally activated selfhealing system based on the DA reaction of synthesized furan-maleimide polymers. Plaisted & Nemat-Nasser (2007) demonstrated increased healing efficiency and the repeatable healing of a similar furan-maleimide polymer.

Crosslinked polymeric materials, which exhibit thermal remendability and removability through Diels-Alder (DA) and retro-DA reactions, were obtained from using multifunctional furan and melamine-based as monomers (Liu & Hsieh, 2006). Liu & Hsieh (2006) reported a similar cross-linked polymer constructed from the tris-maleimide (TMI) and tris-furan (TF) monomers. The reaction scheme and SEM

images were presented as DA and RDA reactions in Figure 1.8 and Figure 1.9 respectively.

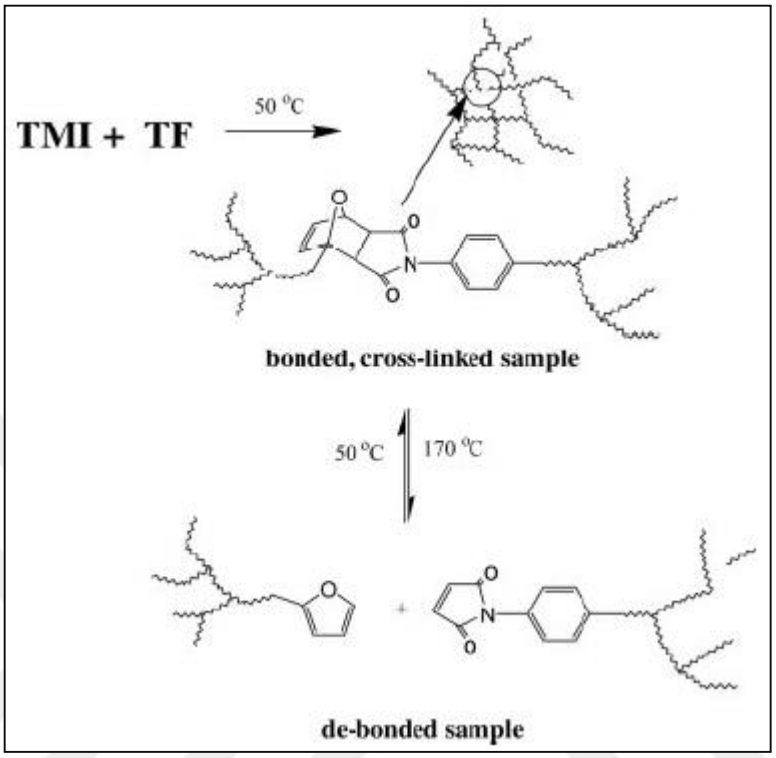

Figure 1.8 Thermally reversible crosslinking reaction of TMI and TF through DA and retro-DA reactions (Liu & Hsieh, 2006).

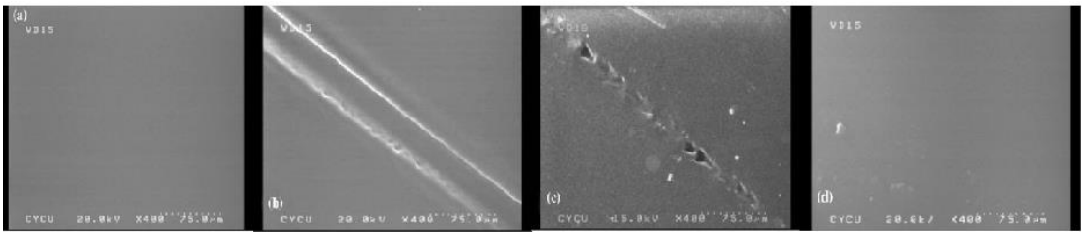

Figure 1.9 SEM micrographs of (a) pristine crosslinked polymer, (b) knife-cut sample, (c) thermally mended sample (50 ºC; 12 h), and (d) thermally mended sample (50 ºC; 24 h) (Liu & Hsieh, 2006).

1.2.2.2 Self-healing From Dispersed Thermoplastic Polymers

Self-healing in thermoset materials can be achieved by incorporating a meltable thermoplastic additive. Self-healing occurs by the melting and subsequent redispersion of the thermoplastic material into the crack plane, filling the crack and mechanically interlocking with the surrounding matrix material (Blaiszik et al.,

2010). Hayes, Zhang, Branthwaite, & Jones (2007); Hayes, Jones, Marshiya, & Zhang (2007) showed that incorporation of a dispersed thermoplastic resin, linear poly(bisphenol-A-coepichlorohydrin), into an epoxy composite reduced delamination area, eliminated matrix cracking, allowed for recovery of load bearing after thermal healing, and allowed for multiple healing cycles. Luo et al. (2009) prepared a thermally remendable thermoset epoxy resin by dispersing phase-separated poly(caprolactone) (PCL) in an epoxy matrix. Upon heating, the PCL melts and undergoes a volumetric thermal expansion to fill the damage.

1.2.2.3 Ionomeric Self-healing Materials

Ionomeric copolymers are a class of materials with ionic segments that can form clusters that act as reversible cross-links as shown in Figure 1.10. These clusters can be activated by external stimuli such as temperature or ultraviolet (UV) irradiation. Because the formation of the clusters is reversible, multiple local healing events are possible. Projectile testing of poly(ethylene-co-methacrylic acid) (EMAA) copolymers with ionic segments was conducted by Kalista, Ward, & Oyentunji, 2007; Kalista & Ward, 2007 and investigated further by Varley & van der Zwaang, 2008. The heat generated during projectile damage served as the trigger for self-healing in these cases.

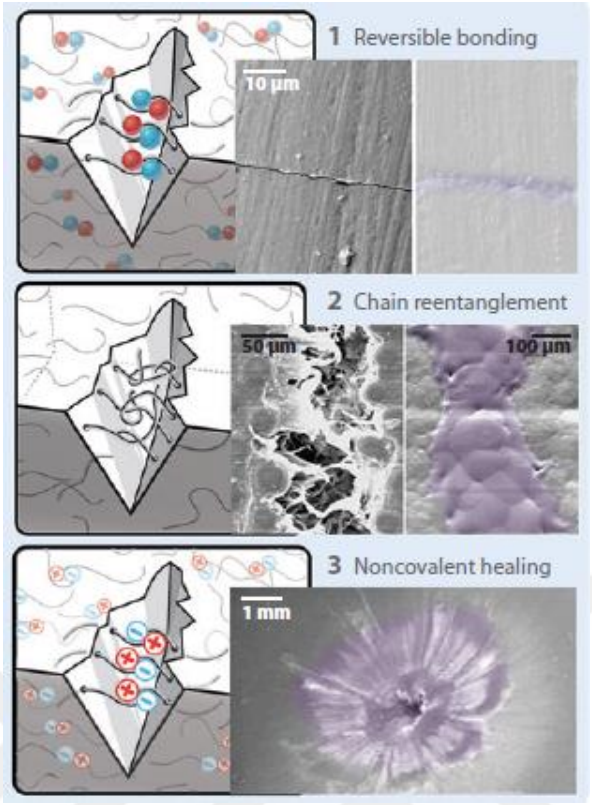

Figure 1.10 Intrinsic self-healing materials (Blaiszik et al., 2010).

Ghosh & Urban (2009) reported the development of polyurethane networks that exhibit self-repairing characteristics upon exposure to ultraviolet light as shown in Figure 1.11. The network consists of an oxetane-substituted chitosan precursor incorporated into a two-component polyurethane. Upon mechanical damage of the network, four-member oxetane rings open to create two reactive ends. When exposed to ultraviolet light, chitosan chain scission occurs, which forms crosslinks with the reactive oxetane ends, thus repairing the network. These materials are capable of repairing themselves in less than an hour. It can be used in many coatings applications. The reaction scheme was composed of two steps and presented in Figure 1.12. In the first step, Oxetane-Chitosan was the synthesized by the reaction of primary alcohol of Chitosan and chloromethyl of Oxetane (Wan, Creber, Peppley, & Bui, 2004). The second step illustrates the reactions leading to the incorporation of Oxetane-Chitosan into trifunctional hexamethylene diisocyante (HDI) in the presence of polyethylene glycol (PEG).

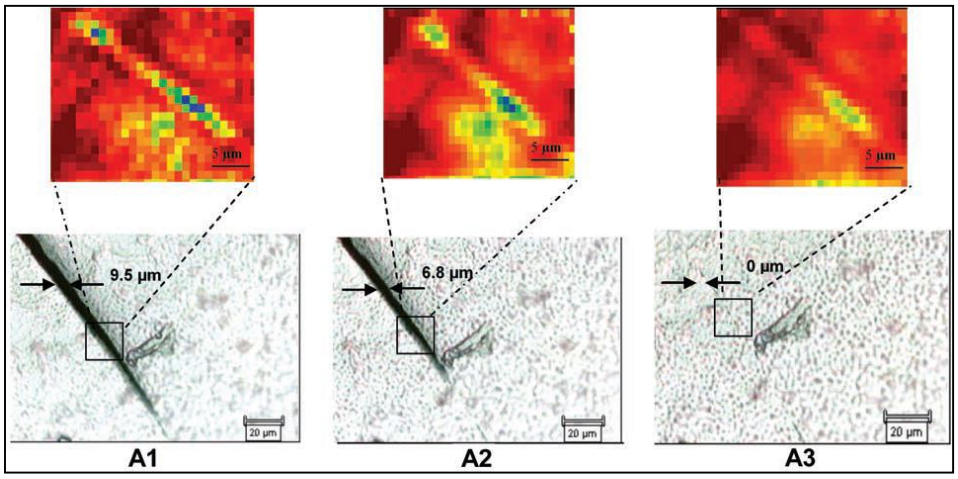

Figure 1.11 IR (upper) and optical (lower) images of Oxetane-Chitosan-Polyurethane networks recorded as a UV exposure time. A1, 0 min; A2, 15 min; A3, 30 min. (SOM provides details regarding spectroscopic changes detected by IR imaging.) (Ghosh & Urban, 2009).

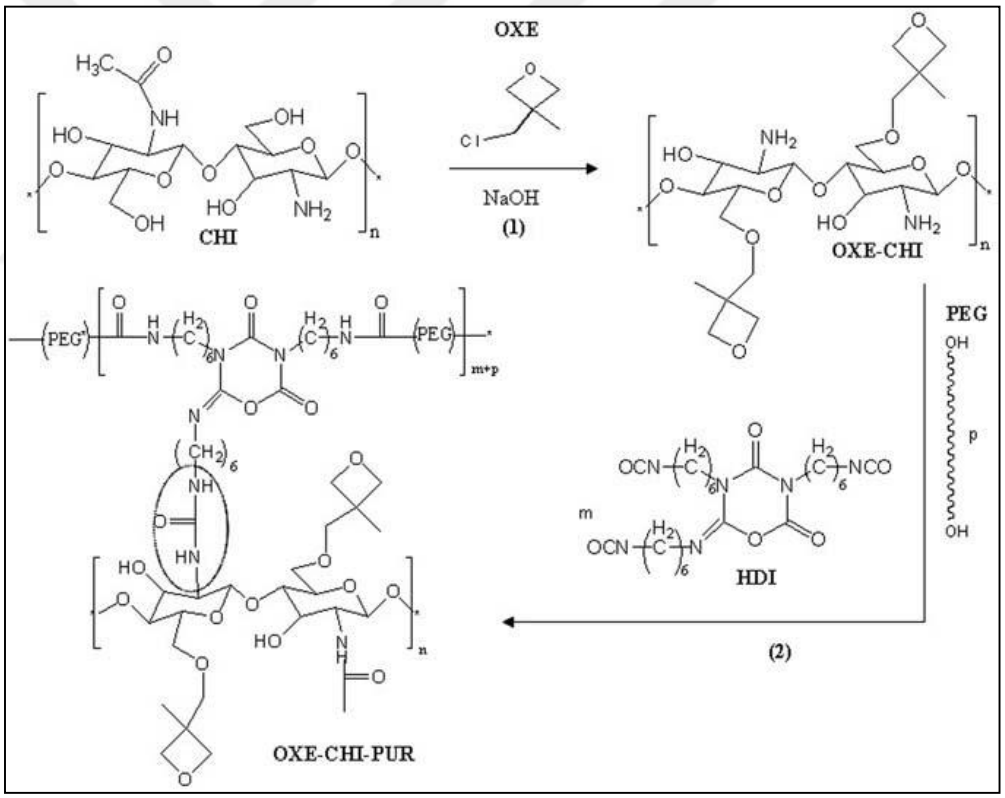

Figure 1.12 Synthetic steps involved in the formation of Oxetane-Chitosan, (1) Reactions of Oxetane with Chitosan leading to the formation of Oxetane-Chitosan precursor; (2) Reactions of Oxetane-Chitosan with HDI and PEG, leading to formations of remendable Oxetane-Chitosan-Polyurethane network (Ghosh & Urban, 2009)

1.2.2.4 Supramolecular Self-healing Materials

Polymers can be designed to form strong end group and/or side-group associations via multiple complementary, reversible hydrogen bonds, resulting in a self-healing elastomeric polymer (Blaiszik et al., 2010). Cordier et al. (Cordier, Tournialhac, Soulie-Ziakovic, & Leibler, 2008) demonstrated self-healing of a rubbery material prepared via supramolecular assembly. Montarnal et al. (Montarnal, Tournilhac, Hidalgo, Couturier, & Leibler, 2009) also developed precursor molecules for the same system. After these, rubbery selfhealing materials were damaged, the pieces may be brought back into close contact to allow for reformation of the hydrogen bonds.

1.2.3 Vascular Self-Healing Materials

In recent years, self-healing utilizing healing agents delivered to the damage by an embedded vascular network that has multiple dimension connectivity. The process in called as vascular healing and given schematically in Figure 1.13. In this process, the self-healing materials sequester the healing agent in a network in the form of capillaries or hollow channels, which may be interconnected until damage triggers self-healing (Blaiszik et al., 2010).

Two main techniques were given in this vascular self-healing process. These network structures for self-healing were given in the following as in:

1- Hollow glass tubes and glass fibers

2-Three-dimensional miscovascular networks

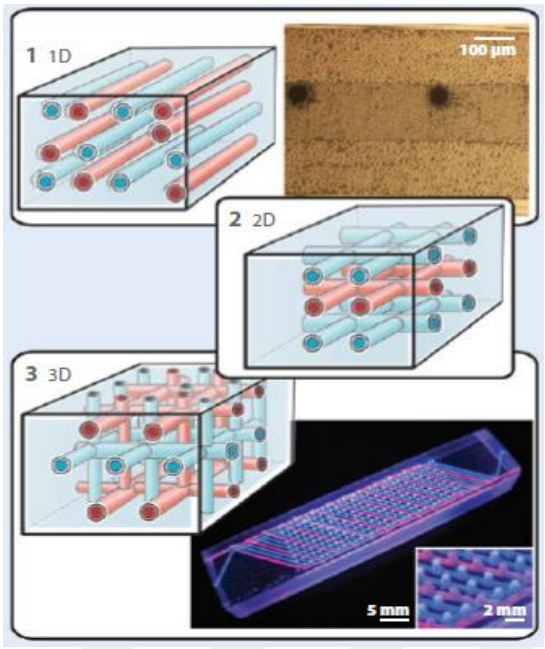

Figure 1.13 Vascular self-healing materials (Blaiszik et al., 2010).

One-dimensional (1D) networks are obtained from hollow channels/fibers filled with healing agent(s). The carbon fiber/epoxy laminate with hollow glass fibers containing a two-part epoxy healing agent was given as an example in Figure 1.14. Dry and Sottos (1993); Dry (1996) carried out initial investigations into self-healing 1D systems. The researchers qualitatively examined the healing ability of epoxies with millimeter-diameter glass pipettes preloaded with either cyanoacrylate or a separated twopart epoxy system. Motuku et al. (1999) further explored the use of pipettes, along with tubes made of several different materials, to evaluate their suitability for incorporation into fiber-reinforced vinyl ester and epoxy resins. The researchers examined the network volume fraction and specimen thickness effects on matrix impact response but did not evaluate the healing ability of the networks. Commercially available 15-µm-diameter HGFs were adopted by Bleay et al. (2001) and were organized into unidirectional plies for composite laminates. Fibers within cured laminate specimens were filled with various fluids using applied vacuum, and release from fibers into damage zones was observed by ultrasonography and X-radiography (Blaiszik et al., 2010).

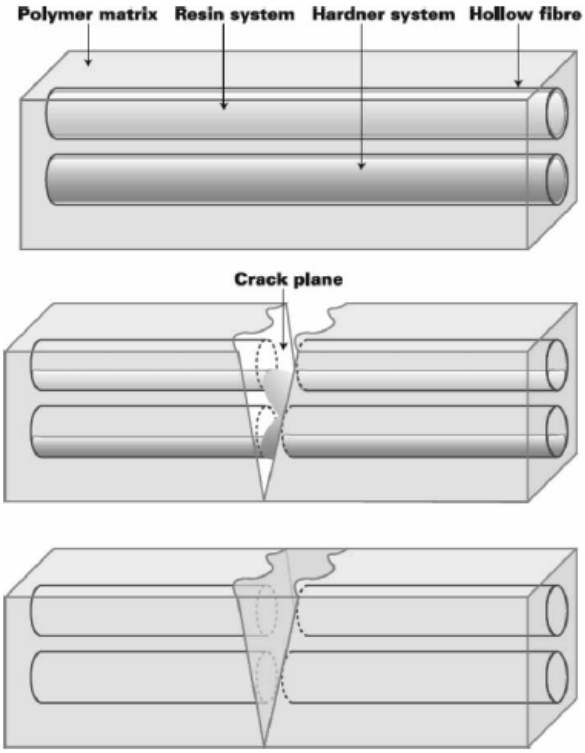

Figure 1.14 Self-healing concept using hollow fibers or tubes (Kessler, 2007)

Two- and three-dimensional (2D and 3D) networks require more sophisticated manufacturing to ensure connectivity. An example of 3D connectivity is the interpenetrating networks containing a two-part epoxy healing agent manufactured using direct-write assembly. Hansen et al. (2009) refined direct-ink writing methods to make complex, isolated interpenetrating networks in order to optimize stoichiometry and to improve mixing for a two-part epoxy healing system and have achieved more than 30 repeated healing cycles.

1.3 The Properties of Chitosan

Chitosan is a polysaccharide obtained by N-deacetylation of chitin in alkaline medium (Dambies, Guimon, Yiacoumi, & Guibal, 2001; Sashiwa, 2005; Verma & Ray, 2005). It consists mainly of β-(1→4)-2-acetamido-2-deoxy-D glucose units. Chitosan is a copolymer of N-acetyl D glucosamine and D glucosamine and the second most abundant biopolymer on Earth after cellulose (Dutta, Chattopadhyaya, & Tripathi, 2004; Mathur & Narang, 1990). Molecular structure of chitin and chitosan are given in Figure 1.15a.

Chitosan is commonly prepared by deacetylation of α-chitin using 40-50% aqueous alkali solution at 100-160°C for a few hours. The resulting chitosan has a degree of deacetylation (DA) up to 0.95. The reaction scheme is given in Figure 1.15b.

Chitosan becomes soluble in aqueous acidic media. The solubilization occurs by protonation of the NH_2 functional group on the C-2 position of the D-glucosamine repeating unit, whereby the polysaccharide is converted to a polyelectrolyte in acidic media.

The presence of NH_2 groups in chitosan is the reason why it exhibits much greater potential compared with chitin for use in different applications. It is a special biopolymer having good properties such as biodegradability, biocompatibility, and antibacterial activity so it is interesting as a novel type of functional material. Chitosan is the only pseudo natural cationic polymer and thus has many applications in different fields (Kurita, 2001; Rinaudo, 2006).

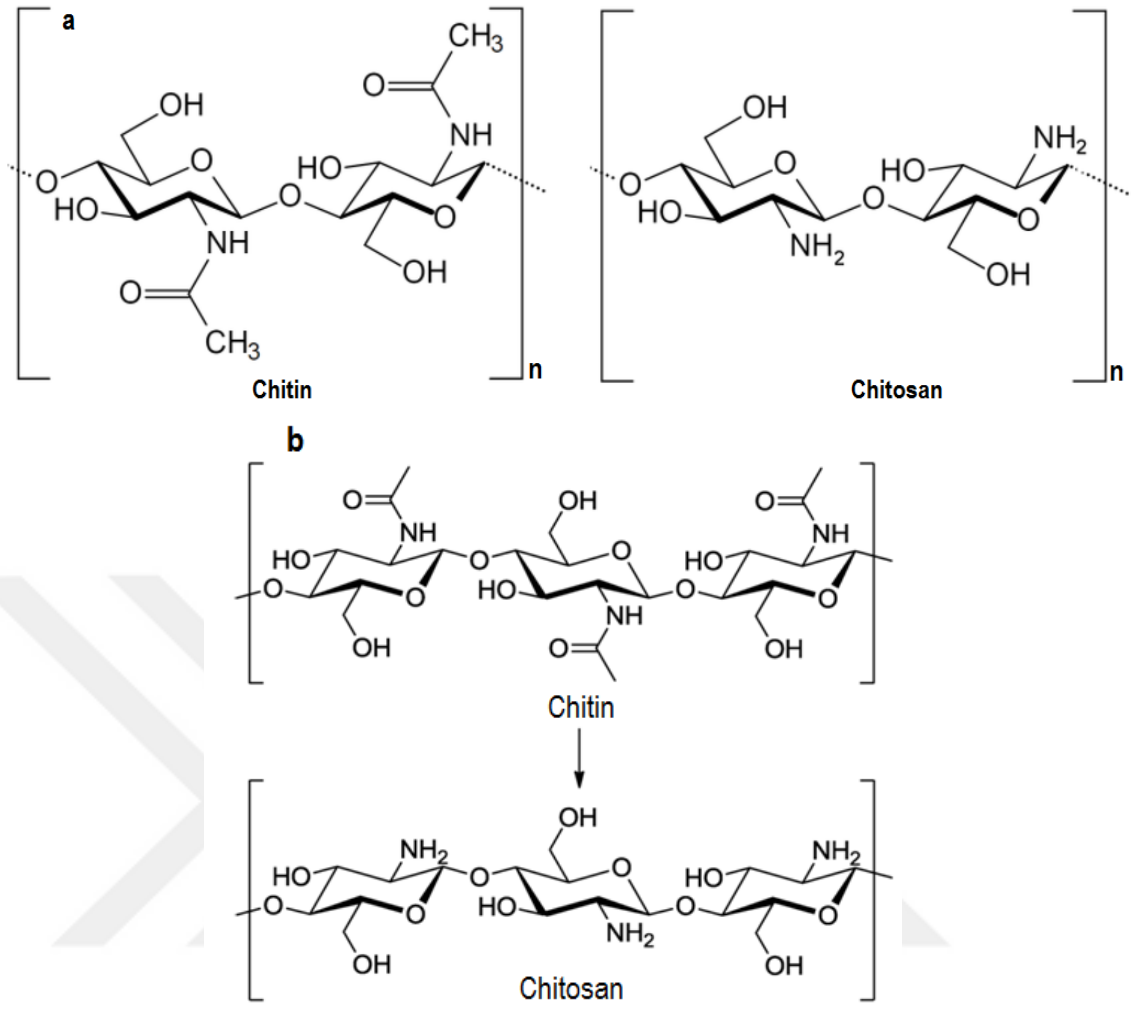

Figure1.15 a) Structures of Chitin and Chitosan b) Deacetylation of chitin to chitosan

There are also problems in using chitosan. One of them is that it is difficult to dissolve in water and neutral pH range. However, when chemical modifications change the fundamental skeleton of chitosan, the modified chitosan lost the original physicochemical and biochemical activities. On the other hand, the chemical modifications of chitosan may have an advantage, because the modification with a hydrophilic reagent would be expected to result in hydrophilic chitosan while keeping the fundamental skeleton intact. Some approaches for the graft reaction of hydrophilic reagent onto chitosan was reported as a technique to improve the affinity to water or organic solvents (Sugimoto, Morimoto, Sashiwa, Saimoto, & Shigemasa, 1998).

Chitosan has $–NH_2$ and –OH functional groups that can chelate heavy metal ions. Therefore, it can be used as adsorbent for providing high adsorption capacity and selectivity againt metal ions (Findon, McKay, & Blair, 1993).

Modification of Chitosan over the $–NH_2$ and –OH functional groups makes it very useful. As an example, N-alkyl chitosan derivatives were prepared by introducing alkyl groups into the amine groups of chitosan via Schiff's base intermediates as shown in Figure 1.16 (Jia, Shen, & Xu, 2001). Quaternization of the N-alkyl chitosan are also possible to produce water soluble derivatives. It was carried out by using methyl iodide to form cationic polyelectrolytes (Kim, Choi, Chun & Choi, 1997).

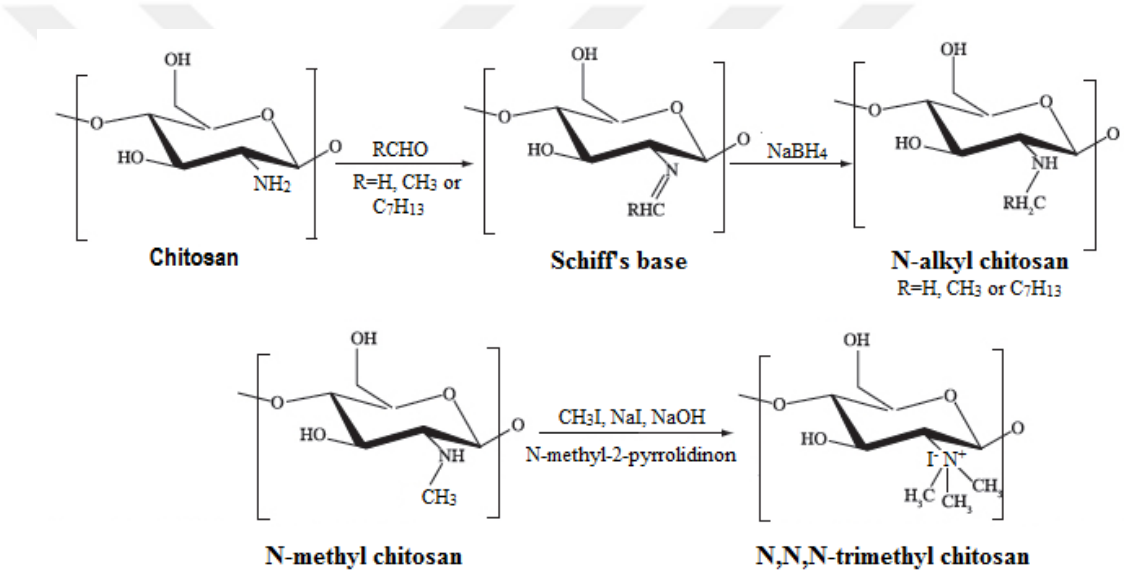

Figure 1.16 The synthesis of N-alkyl chitosans (Jia, Shen, & Xu, 2001; Muhizi, Grelier, & Coma, 2009; Coma, 2013).

Teramoto, Arai & Shibata (2006) reported the synthesis of 4,6,4',6'-O-difurfurylidene-α,α-D-trehalose (DFTreh) was synthesized by acetalization of trehalose with furfural. Diels-Alder polyadditions of DFTreh with 4,4'-bismaleimido-diphenylmethane (BMIDP) and 1,6-bismaleimidohexane (BMIH) were achieved by the reaction at 40-70 °C in DMF. The polymer was found to be almost completely decomposed into corresponding monomers at around 140 °C. The BMIDP which was generated by the degradation of 1 precipitated out from the DMF solution due to homo-polymerization on the prolonged heating at 140 °C, although almost no change

was observed for the case of the BMIH generated from 2 at the same condition. The raection mecanism was given at Figure 1.17.

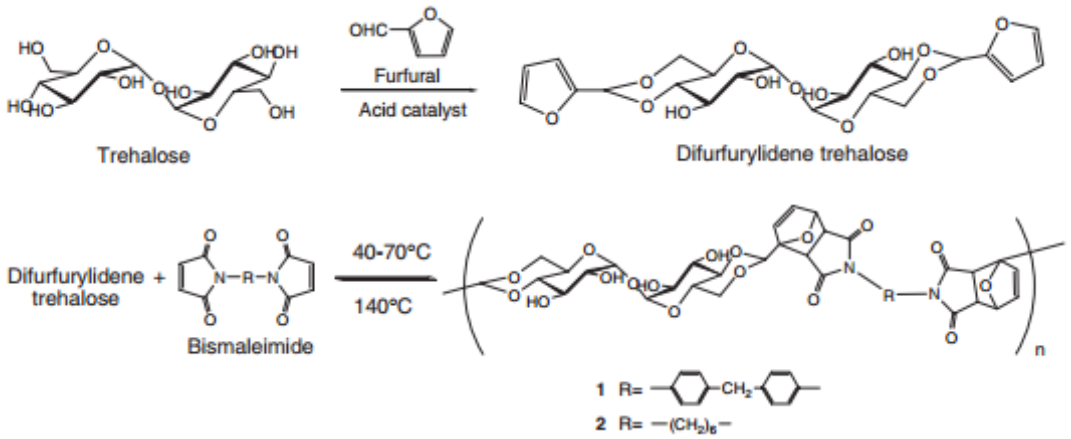

Figure 1.17 Reaction mechaimsm of synthesis of 4,6,4',6'-O-difurfurylidene-α,α-D-trehalose (DFTreh) (Teramoto, Arai & Shibata, 2006).

1.4 Self-Healing Based on Diels-Alder Reaction

The Diels–Alder cycloaddition reaction is one of the most important reactions in organic chemistry. In these reactions, two carbon–carbon bonds in a specific manner forms a cyclic (bicyclic) product. The reaction mechanism is shown in Figure 1.18. The Diels-Alder reaction is a cycloaddition of dienes and dienophiles.

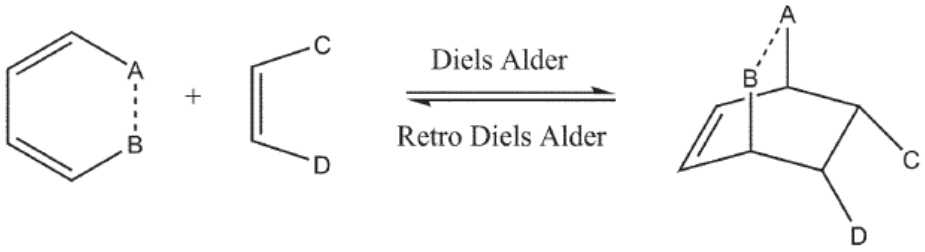

Figure 1.18 Diels-Alder Reaction Mechanism (Bergman & Wudl, 2008).

Two types of reversible polymer have been fabricated: (i) polymers where the pendant groups cross-link through successive DA coupling reactions and (ii) polymers where the backbone itself is constructed through successive DA coupling reactions involving multifunctional complementary monomers. Both types of polymer can revert to their precursors through the RDA reaction and this feature can

be applied in recycling and mending. While a substantial amount of work has been published concerning fabrication of reversible DA-based polymers, only recently has the healing ability of such polymers been demonstrated (Bergman & Wudl, 2008). This reaction has been used to synthesize many novel macromolecules and smart polymeric materials (Bergman & Wudl, 2008; White et al., 2001). At elevated temperatures, a retro-DA (rDA) reaction occurs in which the adduct breaks to form the original furan and maleimide.

Furan-maleimide based polymers have recently been reviewed (Gandini, 2005). Probably the earliest report of incorporation of furan-maleimide moieties into polymers for the purpose of achieving thermal reversibility was reported in 1969 (Craven, 1969). Since then several patents and journal articles have been published, all concerning the fabrication of a thermally reversible polymer network bearing DA-reactive furan and maleimide units, either as pendant groups (for reversible cross-linking), or as part of the polymer backbone (for reversible polymerization).

1.5 The Aim of the Thesis

In this Thesis, the definition and concepts of self-healing in polymeric structures and materials were be examined by using two different healing mechanisms, Capsule based-Autonomic and Intrinsic Self-Healing. Encapsulated polymeric matrixes with reactions such as ROMP. The reactions scheme and the proposed reactions are shown below as Figure 1.19. In this image, we define the proposed mechanism that will be followed in the first part of the thesis.

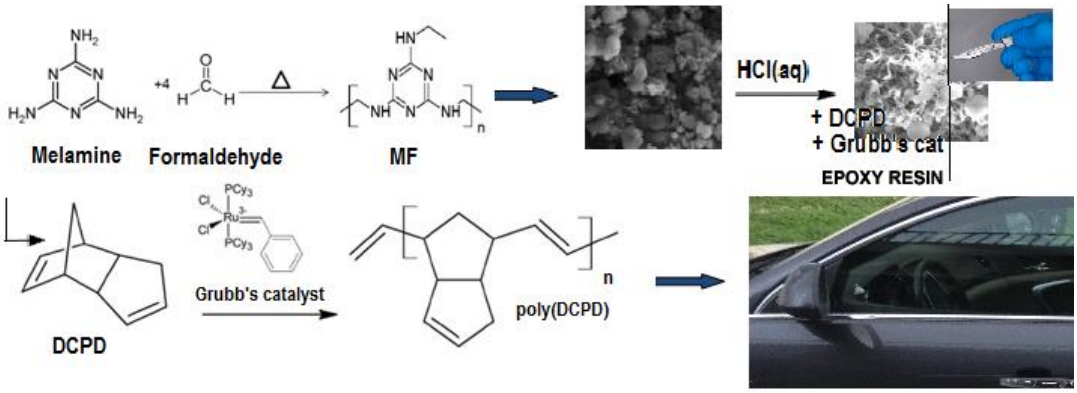

Figure 1.19 A schematic of presentation of the aim of the study: MF microcapsules, Grubbs-catalyzed ROMP of DCPD, pDCPD in the crack on the epoxy resin matrix in the first part.

As can be seen from the Figure 1.19 that for effective and a truly self-healing, DCPD in the MF microcapsules must be able to flow between the crack planes in the material and polymerize by the way of Grubbs' catalyst there under ambient conditions.

The the second part is composed of the thermoreversible reaction for intrinsic self-healing which was carried out as the application of [4 + 2] Diels-Alder reaction DA-rDA. The prepared samples were characterized by several analyses such as FTIR, SEM and ^{1}NMR. As applications, coatings onto glass substrates were prepared. Then they were scratched to see if there is repair in the process by curing the polymer structures.

Thermal behavior of the samples were also examined by using TG/DTA and DSC techniques. Healing observations were carried out by using OM. In the study, chitosan which has a wound healing property is used to see whether it creates a synergetic healing effect or not.

CHAPTER TWO
MATERIALS AND METHODS

2.1 Capsule-Based Self-Healing

2.1.1 Materials

Melamine (Aldrich M2659) and formaldehyde (Aldrich F15587) used as shell-forming materials. Sodium dodecylbenzenesulfonate (SDBS) (Aldrich 289957) used as an emulsifier in the synthesis. Poly(vinyl alcohol) (PVA) (Sigma-Aldrich 363065) used to protect the formed colloid. $NaCO_3$ and HCl aqueous solutions were used to control the pH of the medium. DCPD (Aldrich 454338) was used as core material. Resorcinol (Sigma-Aldrich 398047) was used as inhibitor and 2-ocatanol (Aldrich W280100) was used for the elimination of surface bubbles.

Epoxy resin, diluents and deaerators (Dyo Boya Fabrikaları San. Tic. A. Ş.) used as epoxy matrix. Grubbs' catalyst was used for polymerization of DCPD in epoxy matrix.

2.1.2 Preparation of Epoxy Matrix

The epoxy matrix composite (Dyo Boya Fabrikaları San. Tic. A. Ş.) was prepared by mixing 100 parts epoxide resin, 20 parts of diluents, 0.1 parts deaerators with 60 parts curing agent. Self-healing epoxy specimens were prepared by mixing 2.5% (by weight) Grubbs' catalyst (Aldrich 579726, 1st generation) and 10% (by weight) microcapsules with the resin mixture as described above.

2.1.3 Synthesis of Melamine-Formaldehyde (MF) Resins and Microcapsulation of DCPD

Microencapsulated DCPD with melamine–formaldehyde resins was investigated (Yuan, Liang, & Xie, 2007).

The MF preoplymer were synthesized according to the reaction shown in Figure 2.1. The procedure was given shortly. The MF resin was prepared at an F/M molar ratio of 1.75, with a solid content of 49 wt%. The calculated amounts of melamine, formaldehyde, and distilled water were added to the three neck round-bottomed flask equipped with a stirrer. The pH was adjusted to 8.5 with $NaCO_3$ solution after dissolving melamine. Then, the solution was heated to 65 °C. After waiting for 30 min, MF the prepolymer was obtained according to the reaction shown in Figure 2.1. Afterwards, 100 mL of SDBS solution, DCPD and resorcinol were added to the polymer emulsion mixture. The emulsion was then allowed to stabilize for 25 min. 2-octanol and PVA were added to prevent surface bubbles and to protect the formed colloids during the emulsification, respectively. The pH was adjusted again to 4.0 by HCl. At the same time, the emulsion was heated at about 68 °C. The reaction was ended after continuous agitation for 3 h. The capsule slurry was filtered and washed with water for the removal of excess amounts of DCPD. Finally, the product was dried at room temperature for 24 h.

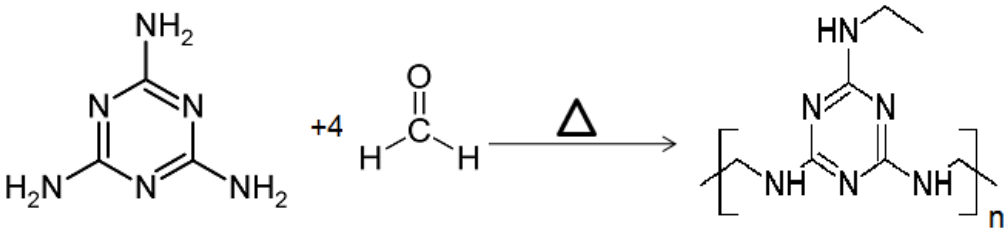

Figure 2.1 Formation of MF prepolymer

2.1.4 Prepar of Epoxy Polymer Coatings

Three different samples and blank were prepared as presented in Table 2.1. The epoxy matrix was composed of 100 parts epoxide resin, 20 parts diluents, 0.1 parts deaerators with 60 parts curing agent and prepared in DYO Paint Factory, Izmir-Turkey. The samples were formed by mixing 2.5% (by weight) Grubbs' catalyst (Aldrich 579726, 1st generation) with 10% (by weight) microcapsules in the resin as stated above. The resin was then coated on glass substrate with a thickness of 200

μm with apparatus, and cured at 80 ºC for 6 h, followed by post curing at room temperature for 24 h. After coating and curing, the mechanical damage was created as scratches. The scratches were carried out under constant load with crosscut knife. Then the healing was observed after heat treatment at 30 ºC and 40 ºC according to the ROMP reaction as shown in Figure 2.2.

All steps were then followed with optical microscope Olympus Model BX60F5 with ×20 magnification.

Table 2.1 Codes and properties of samples

Code	Name	Contents/% weight						Treatment
		Epoxy resin	Diluent	Deaerator	Curing Agent	Catalyst	Capsule	
A	a	100	20	0.1	60	2.5	10	Not filtered
	a/30	+	+	+	+	+	+	Curing for 3h at 30°C
	a/40	+	+	+	+	+	+	Curing a/30 again for 1.5 h at 40°C
B	b	100	20	0.1	60	2.5	10	Filtration/homo geneous/no aggregates
	b/30	+	+	+	+	+	+	Curing for 3h at 30°C
	b/40	+	+	+	+	+	+	Curing b/30 again for 1.5 h at 40°C
C	c	100	20	0.1	60	2.5	10	Solvent addition, 1% MEK
	c/30	+	+	+	+	+	+	Curing for 3h at 30°C
	c/40	+	+	+	+	+	+	Curing c/30 again for 1.5 h at 40°C
K	k	100	20	0.1	60	-	-	Blank sample, dissolved in MEK
	k/30	+	+	+	+	-	-	Curing for 3h at 30°C
	k/40	+	+	+	+	-	-	Curing k/30 again for 1.5 h at 40°C

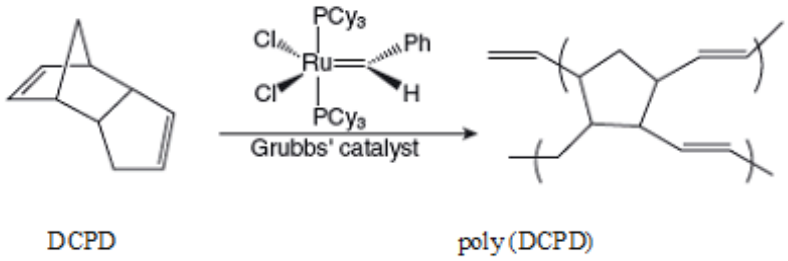

Figure 2.2 Poly(DCPD) formation reaction (White et al., 2001)

2.1.5 Fourier Transform Infrared (FTIR) Spectra of the Samples

FTIR spectra of the samples were carried out on a Perkin-Elmer FTIR spectrophotometer Spectrum BX-II in 4000-400 cm^{-1} with a resolution of 4 cm^{-1}. The samples were prepared as pellets of 1 mg's of dried samples with 100 mg KBr.

2.1.6 SEM Analysis

The surface morphologies of samples were investigated by using Jeol JSM 60 SEM apparatus at 20kV. The samples were coated two times with gold. SEM images were obtained at 50×-5000× magnifications.

2.1.7 Thermal Analysis

Thermal stabilities of the samples were studied by using Perkin Elmer Diamond TG/DTA instrument. The analysis was carried out from 25 ºC to 600 ºC at a heating rate of 15ºC/min under nitrogen flow.

2.2 Intrinsic Self-Healing

2.2.1 Materials

The chemicals such as Chitosan (low viscous, Sigma, 50494), Furfural (Sigma-Aldrich, 185914 , 99%), $NaBH_4$ (Aldrich, 71320), acetic acid (Sigma-Aldrich,

320099, ACS reagent, ≥99.7%), N,N- Dimethylformamide (DMF) (Sigma-Aldrich, 319937) were purchased as commercial products from Sigma-Aldrich and used without further purification.

9-Ethyl-9*H*-carbazole (1), 9-Ethyl-3,6-dinitro-9*H*-carbazole (2), 9-Ethyl-9*H*-carbazole-3,6-diamino (3) were prepared from previously published procedures (Koyuncu, Kaya, Baycan Koyuncu & Ozdemir, 2009; Baycan Koyuncu, Sefer, Koyuncu & Ozdemir, 2011).

2.2.2 Modification of Chitosan

Chitosan solution was prepared by dissolving 1 g chitosan into 5.47 mLs of 1% AcOH. Furfural was added to the chitosan solution at room temperature. After 1h of stirring, the pH of the solution was adjusted to 4.5 by adding 1 M NaOH solution. To this solution, 37.44 mLs of 10% $NaBH_4$ solution was added, and the solution stirred for 1.5 h. The precipitants of N-alkyl chitosan derivatives were obtained by adjusting the pH of the solution to 10. These precipitants were washed several times with distilled water to neutrality and the unreacted aldehyde and the inorganic products were extracted with 1/1(v) EtOH and ether for 5 days in a soxhlet aparatus. The resulting N-alkyl chitosan (CF) derivative was filtered out and dried at room temperature. The reaction mechanism is shown at Figure 2.3 (Jia, Shen & Xu, 2001; Teramoto, Arai & Shibata, 2006; Renbutsu et al., 2005).

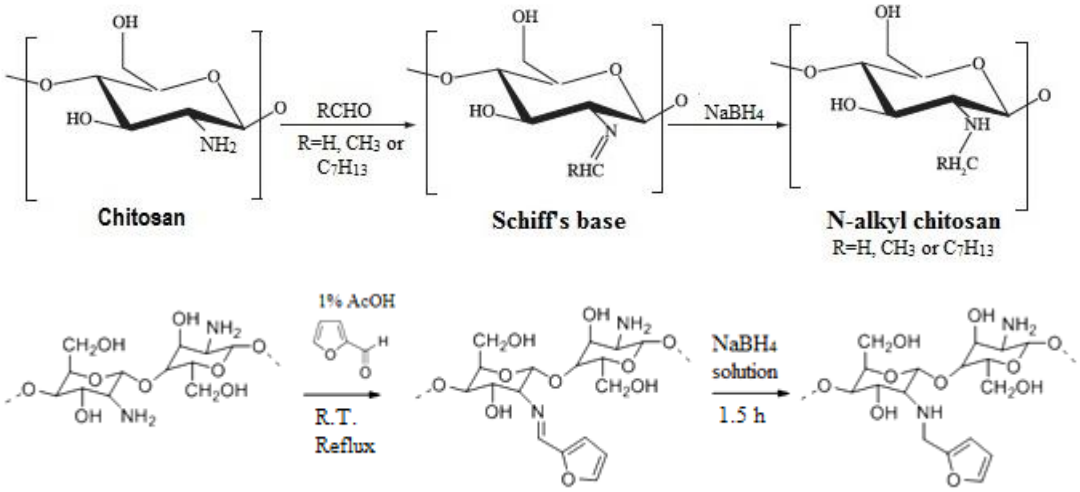

Figure 2.3 The synthesis of N-alkyl chitosan (CF)

2.2.3 Synthesis of Bismaleimide

Bismaleimide (1,1'-(9-Etil-9*H*-karbazol-3,6-diil)bis(1*H*-pirol-2,5-dion) was synthesized from carbazole. The reaction mechanism was given in Figure 2.4. This synthesis had four steps. 9-Ethyl-9*H*-carbazole (1), 9-Ethyl-3,6-dinitro-9*H*-carbazole (2), 9-Ethyl-9*H*-carbazole-3,6-diamino (3) were synthesized, respectively. These compounds were synthesized according to the literature (Baycan Koyuncu, Sefer, Koyuncu & Özdemir, 2011; Koyuncu, Kaya, Baycan Koyuncu & Özdemir, 2009). At the fourth step; we solved maleic anhydride (10.5 mmol) in choloroform. The choloroform solution of 9-Etil-9*H*-karbazol-3,6-diamin was added dropwise in it at room temperature and mixed all night long. The resultant yellow precipitate was filtered and put into a flask. After that sodium acetate and acetic anhydride were added and mixed at 100 °C for 1.5 hours. The reaction mixing was poured in the cold water and mixed all night long. The resulting yellow precipitate was filtered and purified with etil acetate:hexane (1:1) column chromatography on silica gel. 1,1'-(9-Ethyl-9*H*-carbazole-3,6-diil)bis(1*H*-pyrol-2,5-dion) was been synthesized.

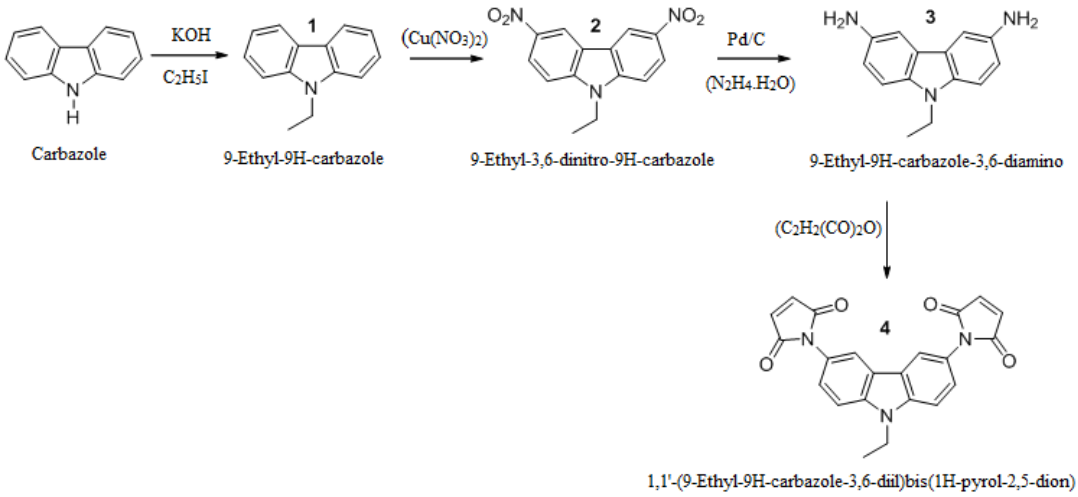

Figure 2.4 The reaction mechanism of (1,1'-(9-Etil-9*H*-karbazol-3,6-diil)bis(1*H*-pirol-2,5-dion)

2.2.4 Diels-Alder Reaction between Bismaleimide and Chitosan-Furan

Different ratio of modified chitosan (CF) and bismaleimide (BMI) were dissolved in %1 acetic acid solution and small amounts of dimethylformamide (DMF), respectively as indicated in Table 2.2. CF solution was filtered and bismaleimide solution was added drop by drop onto CF solution. The mixture was stirred at room temperature for 30 minutes. After that, the mixture was poured in the vials and observed at room temperature. At that time, Diels-Alder reaction occured and liquid form transforms gel formed as in Figure 2.5. Cross-linked gel is based on the Diels-Alder reaction between maleimide groups on a bismaleimide and pendant furans on chitosan. The reaction mechanism was presented in Figure 2.6

Figure 2.5 Photographs show liquid mixture of CF and bismaleimide (left) and cross-linked gel of Diels-Alder reaction (right).

Table 2.2 Reaction Scheme Plan: Chitosan-Furan (CF) and Bismaleimide (BMI)

	MD1	MD2	MD3	MD4	MD5
CF (g)	0.064	0.064	0.064	0.128	0.384
BMI (mg)	4.00	1.99	0.40	0.40	0.24
CF/BMI Mol Ratio	1/100	1/50	1/10	1/5	1/1

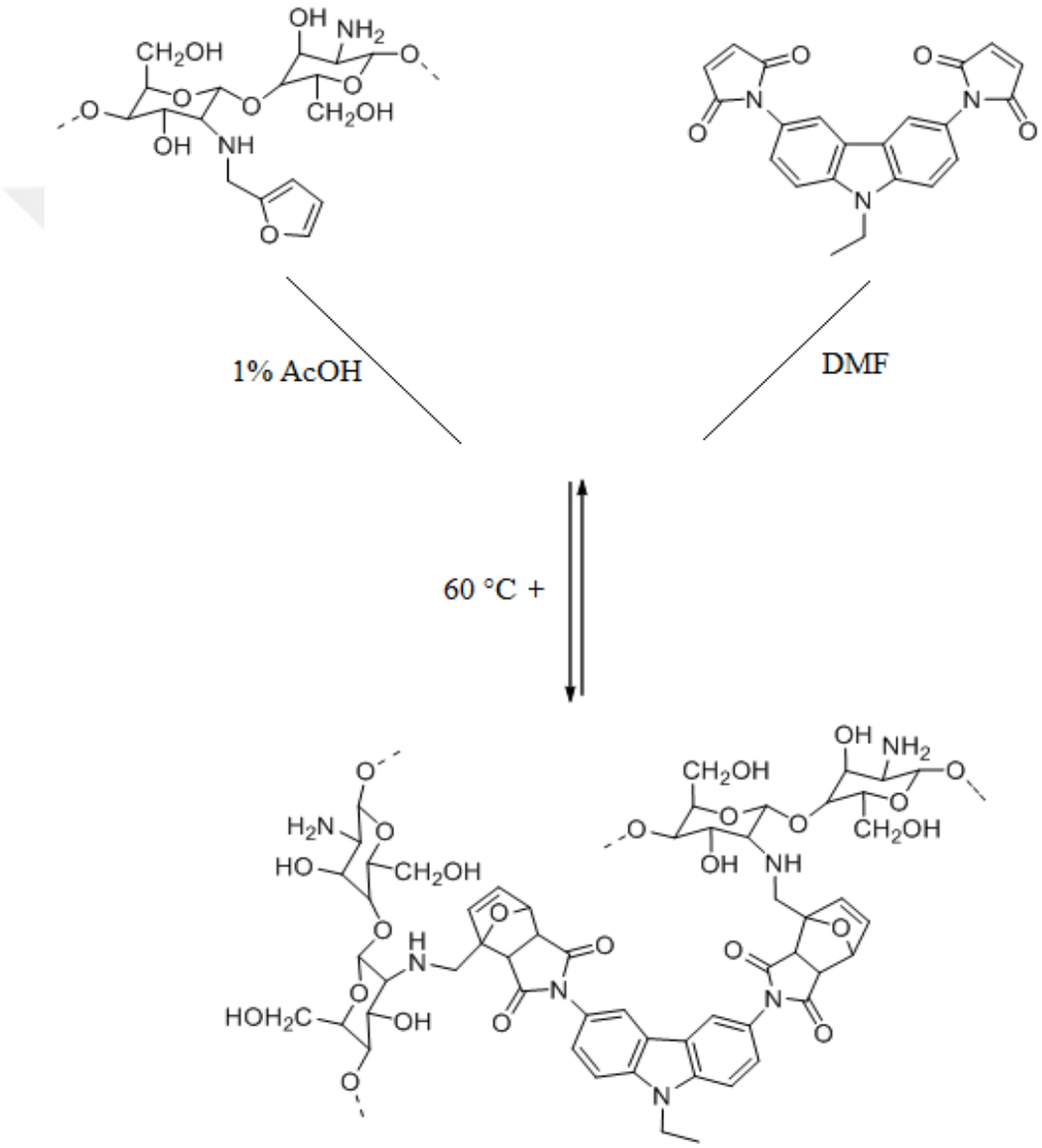

Figure 2.6 Diels-Alder reaction between maleimide groups on a bismaleimide and pendant furans on chitosan

2.2.5 Preparation of Coating Films

We used solvent born technique which composed of two components (2K), polyuretan (PU) system as varnish. First component (varnish) is an acylic polyol based compound and second component (hardener) is a isocyanate. The solvent of the system is *n*-buthyl acetate.

The mixing ratios of varnish/CF solution–BMI solution/hardener are given in Table 2.3. Viscosity and density of varnish/CF-BMI and hardener are given in Table 2.4. The mixtures were applied as 120 μm by applicator on glass panels and cured at room temperature for three days.

Table 2.3 Mixing Ratios of the Varnish/Hardener/CF-BMI

Samples	Varnish/g	CF–BMI/g	Hardner/g
Blanc	77	-	40
MD1V	77	2.50	40
MD2V	77	2.57	40
MD3V	77	2.50	40
MD4V	77	3.24	40
MD5V	77	5.61	40

Table 2.4 Varnish and Hardener Values

Property/Precursor	Varnish / CF-BMI	Hardener
Viscosity (s) DINCUP4	47"	11"
Density (g/cm^3)	0.98	0.95

2.2.6 Fourier Transform Infrared (FTIR) Spectra of the Samples

FTIR spectroscopy was used to obtain the information about the interactions between chitosan and furfural. For this purposes, 1 mg's of chitosan, furfural and CF

were mixed with 100 mg KBr after dried at 60 ºC. FTIR spectra of the samples were then taken as KBr pellets by using Perkin-Elmer BX-II FTIR spectrophotometer.

2.2.7 ^{1}H-NMR Spectrum of the Samples

^{1}NMR spectroscopy were used to identify the chemical structure of the modified chitosan and (1,1'-(9-Etil-9*H*-karbazol-3,6-diil)bis(1*H*-pirol-2,5-dion) (BMI).The H-NMR spectrum of modified chitosan was recorded on INOVA-600 (16000 Hz). The solvent was deuterated Fluoroaceticacid for modified chitosan and deuterated DMSO for BMI.

2.2.8 Thermal Analysis

The thermal stabilities of CF/BMI blend (S) and CF/BMI Gels (J) were investigated by TG/DTG and DSC analysis under nitrogen flow. For this purpose, gel samples were dried in a freez dryer at -76°C in 0.010 mbar for overnight.

TG analysis were carried out at a temperature range of 25-200 ºC at a heating rate of 15ºC/min for CF/BMI blend (S) and 35-500 ºC at a heating rate of 15ºC/min for CF/BMI gels (J) with Perkin Elmer Diamond TG/DTA instrument.

DSC analysis was performed under nitrogen flow from -20°C to 120°C at a rate of 10°C/min with Perkin Elmer Diamond Differential Scanning Calorimetry (DSC) instrument in Central Research Laboratories of Middle East Technical University/Ankara-Turkey.

2.2.9 Optical Microscope Analysis

Optical Microscopic images were used to investigate the self-healing behavior of the samples. Analysis of the samples was carried out by using Olympus Model BX60F5 OM Microscope with a magnification of 200x in Metallurgical and Materials Engineering Department of Engineering Faculty of Dokuz Eylül University.

CHAPTER THREE
RESULTS AND DISCUSSION

3.1 Capsule-Based Self-Healing

3.1.1 Fourier Transform Infrared (FTIR) Spectra of the Samples

The codes, names and contents of the samples were given in Table 2.1. In Figure 3.1, the spectra of MF wall shell material, DCPD, MF/DCPD capsules and Melamine were presented. In this spectra, DCPD can be characterized by (C=C) and (C–H) stretching vibration bands at 3044 cm^{-1} and at 2959-2842 cm^{-1}, respectively. The (=C–H) bending vibration band was also observed at 1339 cm^{-1}. In the spectrum of MF, the stretching vibration bands of N–H and –OH were observed at 3353 cm^{-1}as overlapping bands. The stretching vibration band of C–N and the bending vibration band of N–H were assigned at 1337-1592-1549 cm^{-1}. The band at 1064 cm^{-1} was for (–C–O–C–) bonds.

The strong absorptions at 2956 and 2873 cm^{-1} represent asymmetric and symmetric stretching frequencies of methylene group of MF resin. Very prominent and strong bands at 1567 and 1492 cm^{-1} can be assigned to the in-plane –C=N- vibrations of the triazine ring system (Loughran, Ehlers, Crawford, Burkett, &Ray, 1964; Padget, & Hammer, 1958). The CH deformation band absorbs at 1453 cm^{-1}, at a low frequency because of the presence of CH group in close vicinity to electronegative nitrogen atom. The band at 1383 cm^{-1} can be assigned to the in-plane CH deformations of heterocyclic rings. A weak band at 1325 cm^{-1} presents C-N stretching vibrations of amino group as substituent on the 1, 3, 5-triazine ring. Stretching frequencies of C-O moiety of alcoholic part of MF resin absorb at 1226, 1154 and 1086 cm^{-1}. These FTIR spectra were supported with the data in the cited references (Padget, & Hammer, 1958; Bhatia, Sarkar, & Alam, 2006).

The IR spectra of MF and CAPSULS showed similar several very distinct bands. The bands at 812 cm^{-1} and bands between 1350 and 1560 cm^{-1} correspond to the

aromatic vibrations of the triazine ring. According to Braun and Legradic's study (Bhatia, Sarkar, & Alam, 2006), the band at 1170 cm^{-1} corresponds to the ether groups. This band is indicative of the methylene ether bridges that form between the triazine rings during polymerization. The band at 1000 cm^{-1} is related to the C-OH bond in hydroxymethyl groups. The broad band between 3000-3500 cm^{-1} is due to the deformation vibrations of $-NH_2$, >NH and –OH groups. IR spectra of MF resin show an intense band at 1560 cm^{-1} related with the triazine ring. This band usually superimposes a bond at 1650 cm^{-1} which is due to C=N stretching vibrations of terminal imino groups formed from $-NHCH_2OR$ groups of the melamine resin (Braun, & Legradic, 1974; Wang, Hu, Cai, & Yu, 2014).

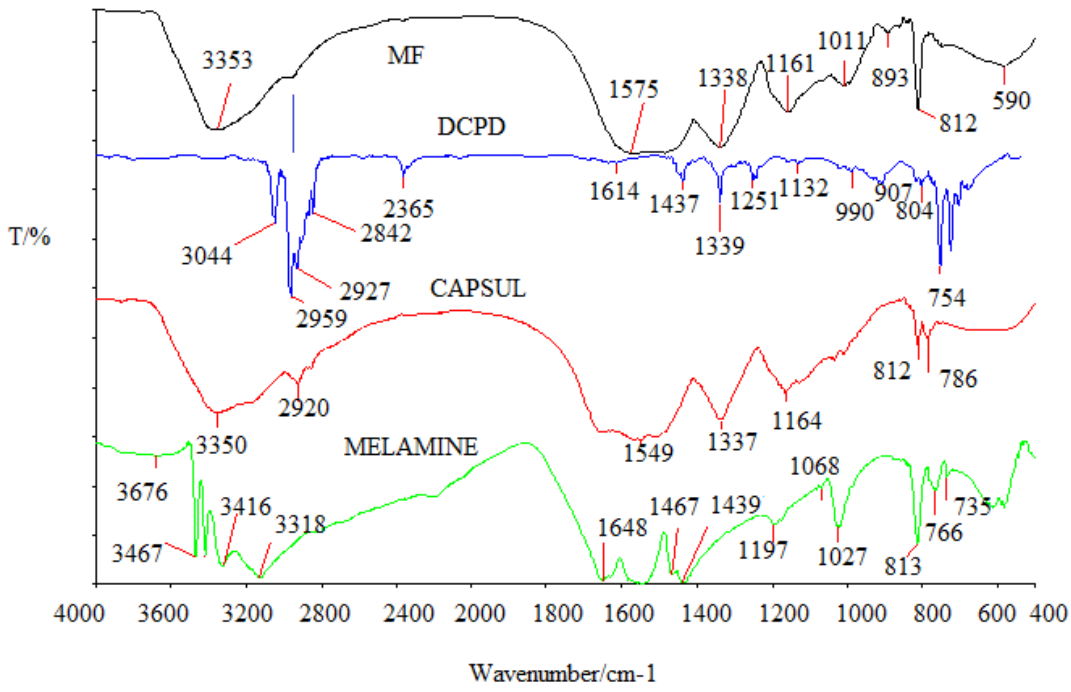

Figure 3.1 FTIR spectra of Melamine, DCPD, and MF wall shell material, and MF microcapsules

3.1.2 Scanning Electron Microscope (SEM) of the Samples

Figure 3.2 shows the SEM micrographs of microcapsules. As can be seen, the microcapsules are spherical in shapes and have smooth surfaces. Aggregates of PMF nanoparticles are also observed in these images.

The self-healing control was observed by using an Optical Microscope with different temperature and time. The images were shown at Figure 3.3-3.6.

In Figures 3.3 and 3.4, it was not observed any change after curing at 40 °C for 1.5 h. On the other hand, it closed with a scratch formed substantially that were restored as seen in Figures 3.5 and 3.6 under same conditions. In other words, it can be said that an improvement in Sample C and K was observed while in other instances, no changes in practice were observed for the other samples in fact. This may be due to the addition of solvent which helps the formation of homogeneous mixture before curing.

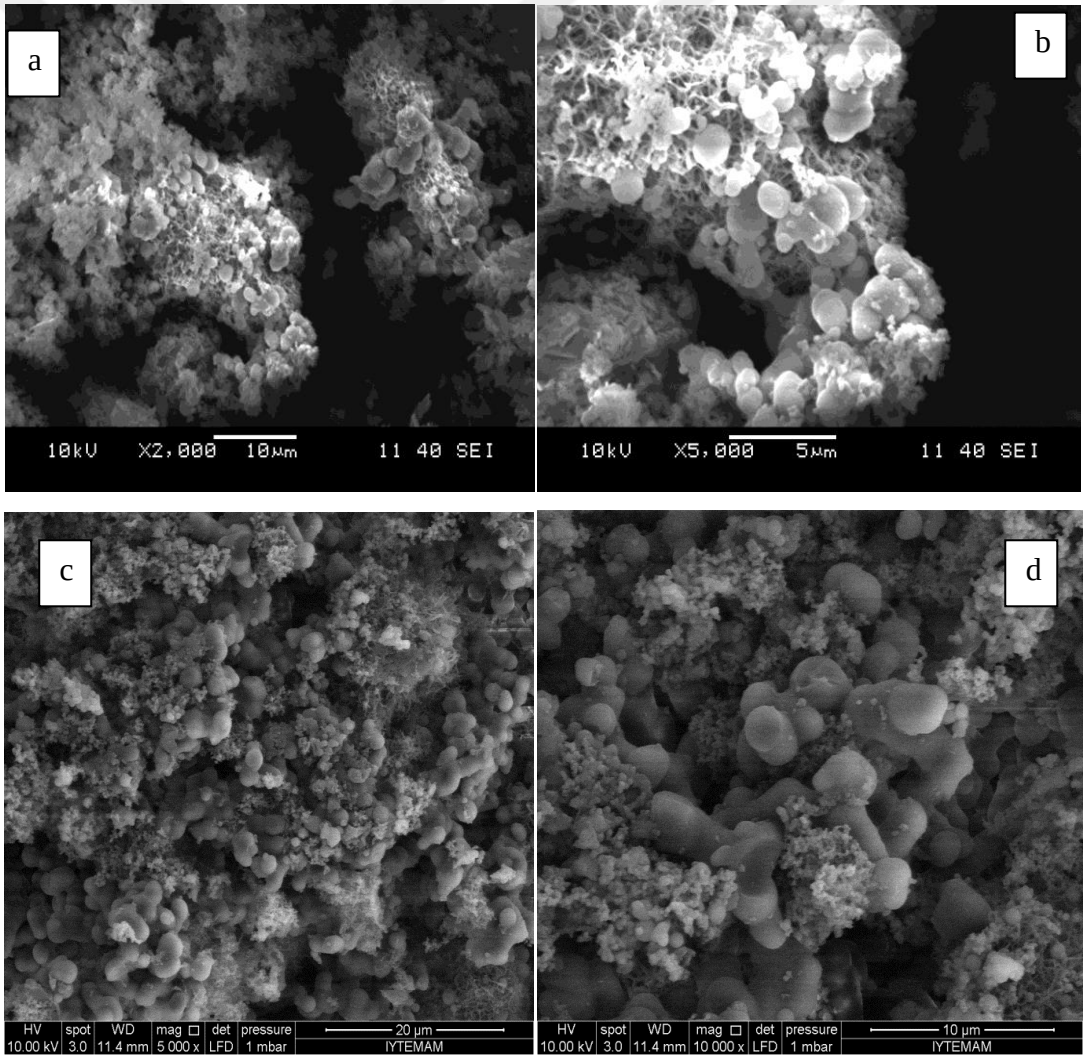

Figure 3.2 SEM micrograph of the microcapsules a) ×2000 b) ×5000 c) ×5000 d) ×10 000

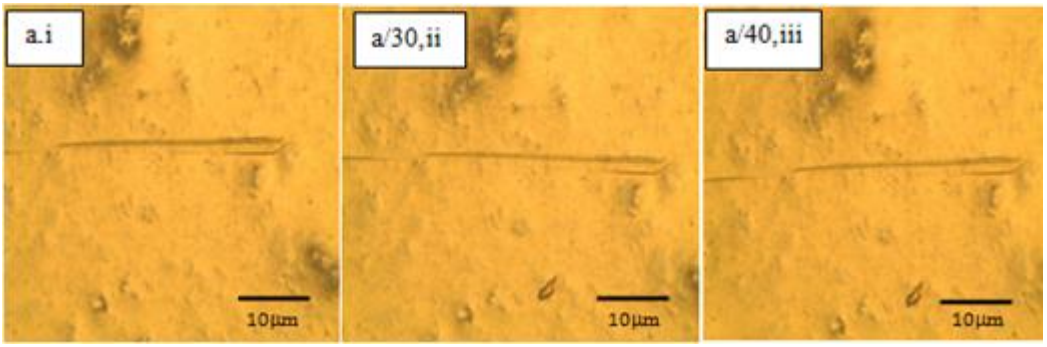

Figure 3.3 OM image of sample A, i) during the scratch was created. ii) after waiting in oven for 3h at 30 ºC. iii) after waiting of ii again in oven for 1.5h at 40 ºC.

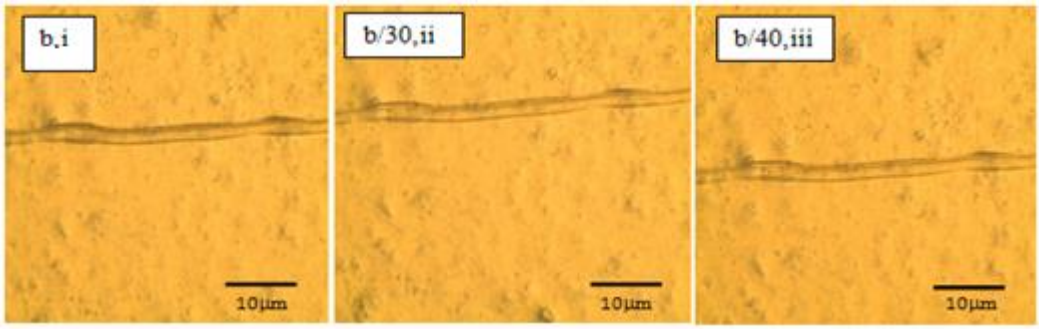

Figure 3.4 OM image of sample B, i) during the scratch was created ii) after waiting in oven for 3h at 30 ºC iii) after waiting in oven for 1.5h at 40 ºC

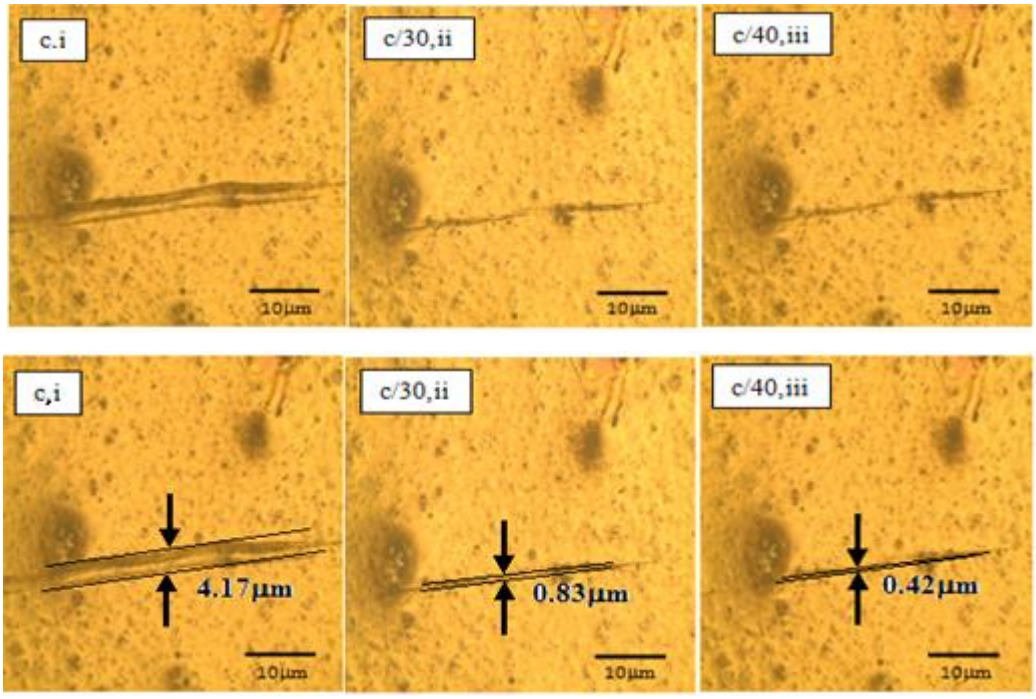

Figure 3.5 OM image of sample C, i) during the scratch was created ii) after waiting in oven for 3h at 30 ºC iii) after waiting in oven for 1.5h at 40 ºC

It is obvious to calculate the healing efficiency from mechanical analysis data, but in our case, the healing efficiency may also be calculated in the following way defined by (Wool & O'Connor, 1981; Wu, Meure, & Solomon, 2008) in Equation 3.1;

$$Healing\ efficiency\ (\eta)/\% = \frac{W_{fg} - W_{ig}}{W_{ig}} x100 \qquad (3.1)$$

Where W_{ig} and W_{fg} are the initial created and final crack gap before and after the healing process. As can be seen from Figure 3.5 for the sample C, W_{ig}, Wf_{g1} and W_{fg2} were 4.17, 0.83 and 0.42µm, respectively. By using Equation 1, the healing efficiency of the sample C was calculated as 80 and 89%.

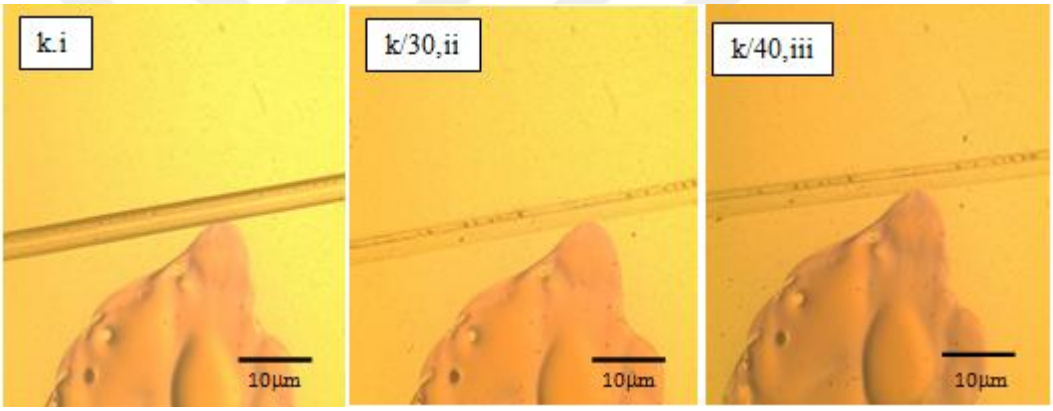

Figure 3.6 OM image of sample K, i) during the scratch was created ii) after waiting in oven for 3h at 30 ºC iii) after waiting in oven for 1.5h at 40 ºC.

3.1.3 Thermal Analysis Results

TG/DTA data of the samples were given on Table 3.1 and 3.2. TGA profiles of the samples are presented in Figure 3.7. DTA thermograms are presented in Figure 3.8. As can be seen from Table 2, the maximum degradation temperature of the samples is about 367°C with an average char yield of 22%. Furthermore, DTA analyses of the thermograms of the polymers exhibit similar degradation feature except sample C.

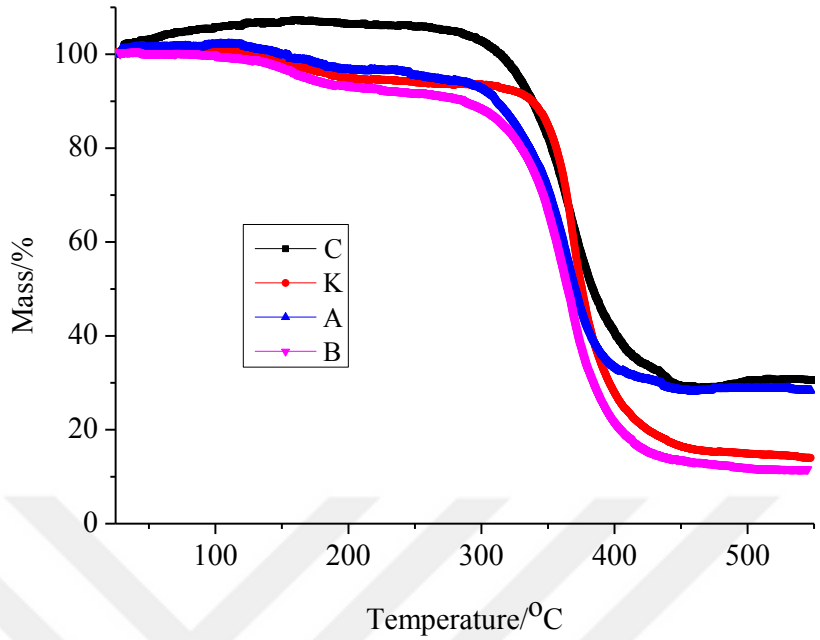

Figure 3.7 TGA profiles of the samples

Table 3.1 TG Analysis data of the samples

TG	Thermograms	
Sample	T_{max}/°C	Mass Loss % 25-550°C
K	369	80
A	365	74
B	368	81
C	364	76
Average	367	78

The curing endotherm of PCPD was an Endo maximum of about 152 °C (Zhang, Sun, Hou, Jie, & Chang, 2006). T_g of the PDCPD is 155°C. The thermal curability of our polymers in which composed of epoxy resin and PCPD was observed at a maximum temperature of 157°C as indicated in Table 3.2 as Endo 2. The third Endo at T_{max} = 375°C is due to the releasing of formaldehyde, methanol, amine, and NH_3 (Ullah et. all, 2014). The cured samples (the bulk polymer) degraded in the range of 400–500 °C with a maximum temperature of 458°C as Endo 4. At Table 3.2 enthalpy values were given J/g type because of molecular weight of polymer did not calculated.

In the DTA thermograms of the sample C, two endotherms as Endo 1, Endo 4 and also weak endotherms as a, b in Figure 3.8 were observed.

Table 3.2 DTA Analysis data of the samples

DTA	1		2		3		4	
Sample	Endo T_{max}/°C	ΔH J/g	Endo T_{max}/°C	ΔH J/g	Endo T_{max}/°C	ΔH J/g	Endo T_{max}/°C	ΔH J/g
K	75	19	157	26	373	35	458	8
A	73	17	157	86	377	98	458	12
B	76	26	157	1	373	54	458	8
C	69	5	a	-	b	-	458	58

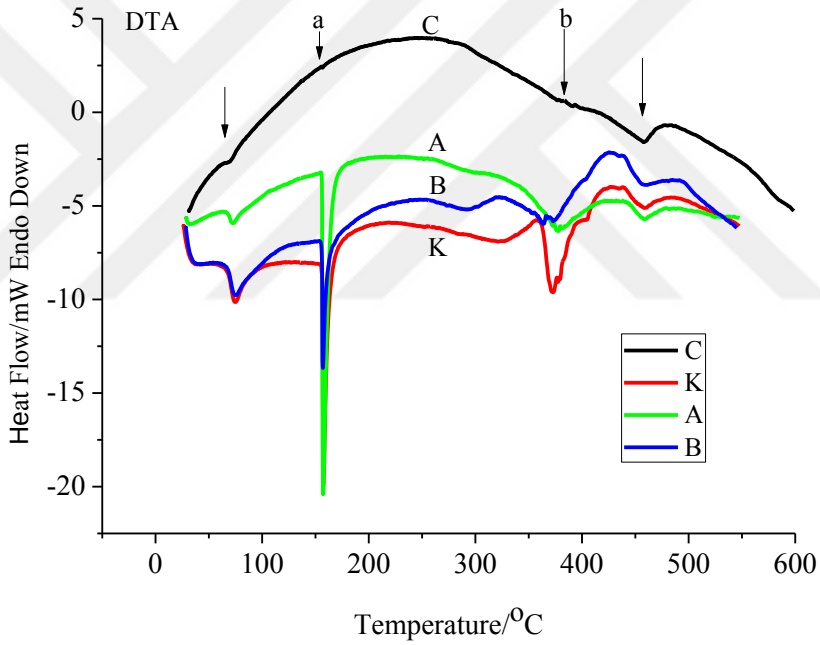

Figure 3.8 DTA Thermograms of the samples

3.2 Intrinsic Self-Healing

3.2.1 Fourier Transform Infrared (FTIR) Spectra of Samples

The chemical structures of chitosan, modified chitosan (CF) and CF/BMI Gels were analyzed by using FTIR spectroscopy. The FTIR spectrum of modified chitosan

was compared with the spectra of chitosan and furfural in Figure 3.9. The FTIR spectra of CF/BMI Gels were also given in Figure 3.10.

According to the literature, the spectrum of furfural shows the characteristic absorption band at 1706 cm^{-1} due to the conjugated carbonyl (C=O). The absorption wavenumber is slightly lower than usual i.e. 1740 cm^{-1} to 1720 cm^{-1} due to internal hydrogen bonding which occurs in conjugated unsaturated aldehydes. Furthermore, the presence of the aldehyde proven with the existence of two bands gained at 2830 cm^{-1} and 2811 cm^{-1}. These absorptions shows a moderate intense stretching of aldehydic C-H which attributes to Fermi resonance between the fundamental aldehydic C-H stretching and the first overtone of the aldehydic C-H bending vibration. It appears at 1393 cm^{-1} in the spectrum. These bands are frequently observed for aldehyde group. However strong bands indicated from 1569 cm^{-1} to 1420 cm^{-1} are stretching of C=C from aromatic ring. Aromatic =C-H bending out of plane bands were observed from 929 cm^{-1} to 883 cm^{-1}. Two strong bands at 1019 cm^{-1} and 1220 cm^{-1} indicated the C-O stretching vibration (Sashikala, & Ong, 2007).

Figure 3.9 shows characteristic bands of furfural and chitosan, seperatly. At the furfural FTIR spectrum, conjugated carbonyl (C=O) absorption band appears at 1683 cm^{-1}. 2849 cm^{-1} and 2812 cm^{-1} show stretching of aldehydic C-H which attributes to Fermi resonance between the fundamental aldehydic C-H stretching and the first overtone of the aldehydic C-H bending vibration. Furthermore the absorption band at 1367 cm^{-1} indicates aldehyde groups. On the other hand, strong bands indicated from 1567 cm^{-1} to 1392 cm^{-1} are stretching of C=C from aromatic ring. Aromatic =C-H bending out of plane bands were observed from 1019 cm^{-1} to 883 cm^{-1}. Two strong bands at 1079 cm^{-1} and 1245 cm^{-1} indicated the C-O stretching vibration.

At the chitosan FTIR spectrum; the main characteristic bands are at 3386 cm^{-1} (-OH and $-NH_2$ stretch); 2875 cm^{-1} (C-H stretch); 1659 cm^{-1} (N-H bend); 1600 cm^{-1} (symmetrical stretch vibration absorption of amino group); 1382 cm^{-1} (C-N stretch); 1155 cm^{-1} (bridge O stretch), and 1075 cm^{-1} (C-O stretch).

Furfural was covalently linked to free amine groups on chitosan, as indicated by the FTIR spectrum of Chitosan-Furan. Chemical cross-linking of the chitosan-furfural blends can be explained by the Schiff base formation as verified by the 1656 and 1560 cm^{-1} bands associated with the C=N and NH_2 groups, respectively. All chitosan-derived blends have shown a relative increase on their imine (-C=N-) band nearly at 1650-1660 cm^{-1} and simultaneous drop on the amine ($-NH_2$) band after chemical cross linking with aldehyde. The imine group was formed by the nucleophilic reaction of the amine from chitosan with the aldehyde. Same sitution is demostrated on the literatures (Costa & Mansur, 2008; Rokhade, Patil, & Aminabhavi, 2007; Wang et al., 2004a; 2004b). The FTIR spectrum exhibits a band at 1474 cm^{-1} which associated with the secondary amines on chitosan, as well as several bands related to the unsaturated carbons (1656, 812 and 740 cm^{-1}) and ether moieties (1153 and 1071 cm^{-1}) of furan rings (Montiel-Herrera et al., 2015; Kumar & Koh, 2012; Kumar, Kim, Grupta, & Dutta, 2012).

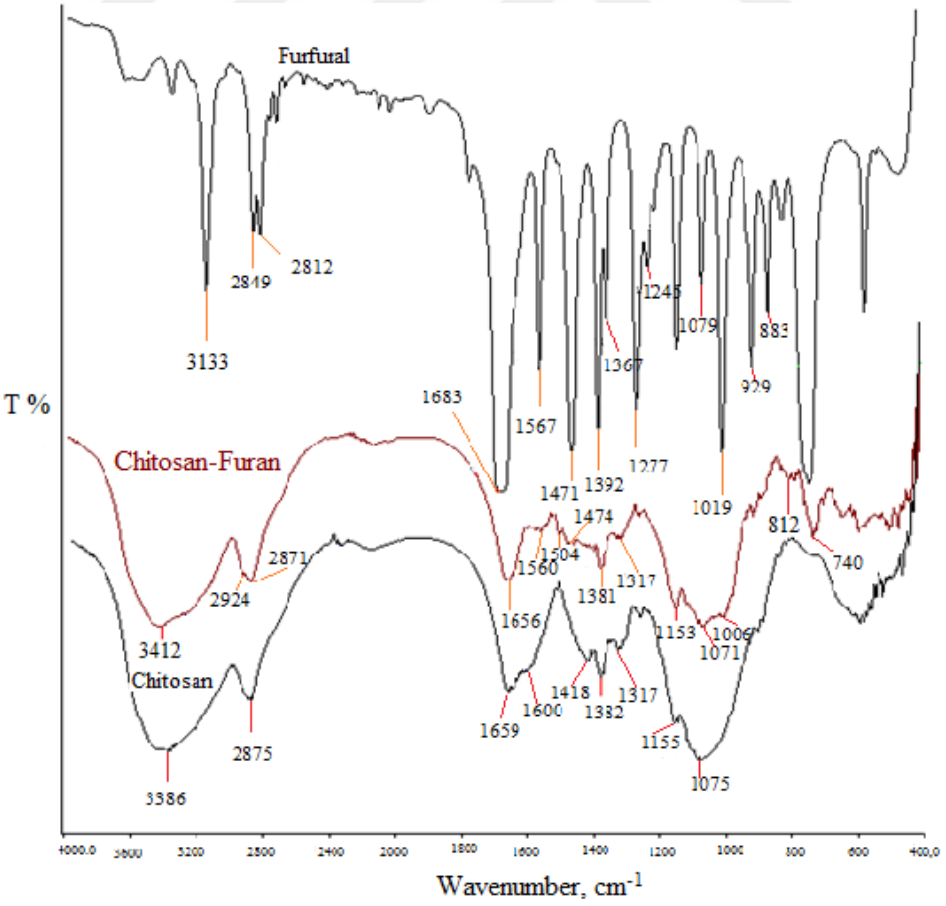

Figure 3.9 FTIR spectra of Chitosan, Chitosan/Furan and Furfural

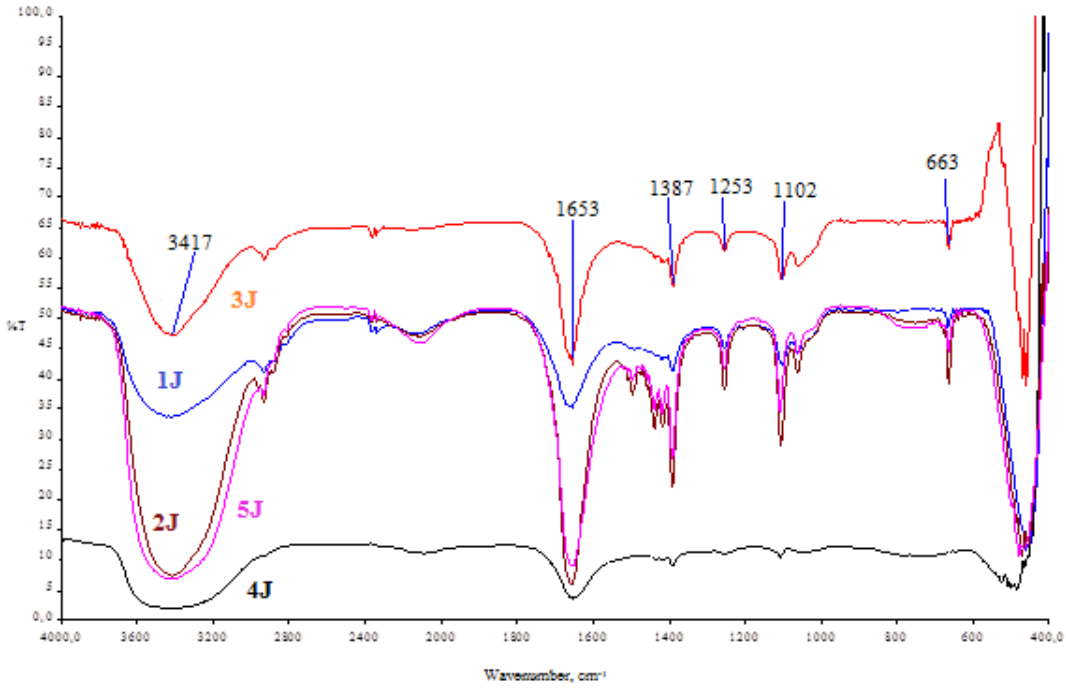

Figure 3.10 FTIR spectra of CF/BMI Gels

3.2.2 ^{1}H-NMR Spectrum of the Samples

^{1}H-NMR spectroscopy was used to identify the chemical structure of the modified chitosan. ^{1}H-NMR spectrum of modified chitosan was compared with the spectra of furfural in Figure 3.11 and ^{1}H-NMR spectra of furfural was presented in Figure 3.12.

The ^{1}H NMR spectrum shows the expected chemical shifts generated by protons bonded to furan rings at Figure 3.11 (Martín-Matute, Nevado, Cárdenas, & Echavarren, 2003). These results corroborated the synthesis of CF (Montiel-Herrera et al., 2015). Other signals were also observed at Figure 3.11 and may correspond to unreacted furfural and Schiff's base form, even when the final product was exhaustively purified by precipitation and 120 h extraction with 1/1(v) EtOH and ether. Totally eleven signals between 6 to 10 ppm. These signals indicate protons bonded to furan rings on CF, protons bonded to furfural and protons bonded to Schiff's base form of furfural. The peaks that are a, b and c indicaded in Figure 3.11 are belonging to protons of furan ring. On the other hand, the peaks that are 2, 3 and

4 are belonging to protons of furfural ring and the other peaks that are between 6 to 10 ppm may belong to Schiff's base form. These peaks were absent in the ^{1}H NMR spectra of furfural. Some degradation of furfural units on the DCH_2FCOOH used as solvent for NMR experiments could not be discarded as well.

The ^{1}H NMR spectrum of the BMI is given in Figure 3.13 The spectrum can be evaluated as: 1.34(t, 3H, J:6.8Hz, CH_3), 4.49(q, 2H, J: 6.8Hz, CH_2), 7.18(s, 4H, =CH), 7.40(dd, 2H, J:8.4Hz, ArH_b), 7.73(d, 2H, J: 8.8Hz, ArH_c), 8.08(d,2H, J:1,6Hz, ArH_a).

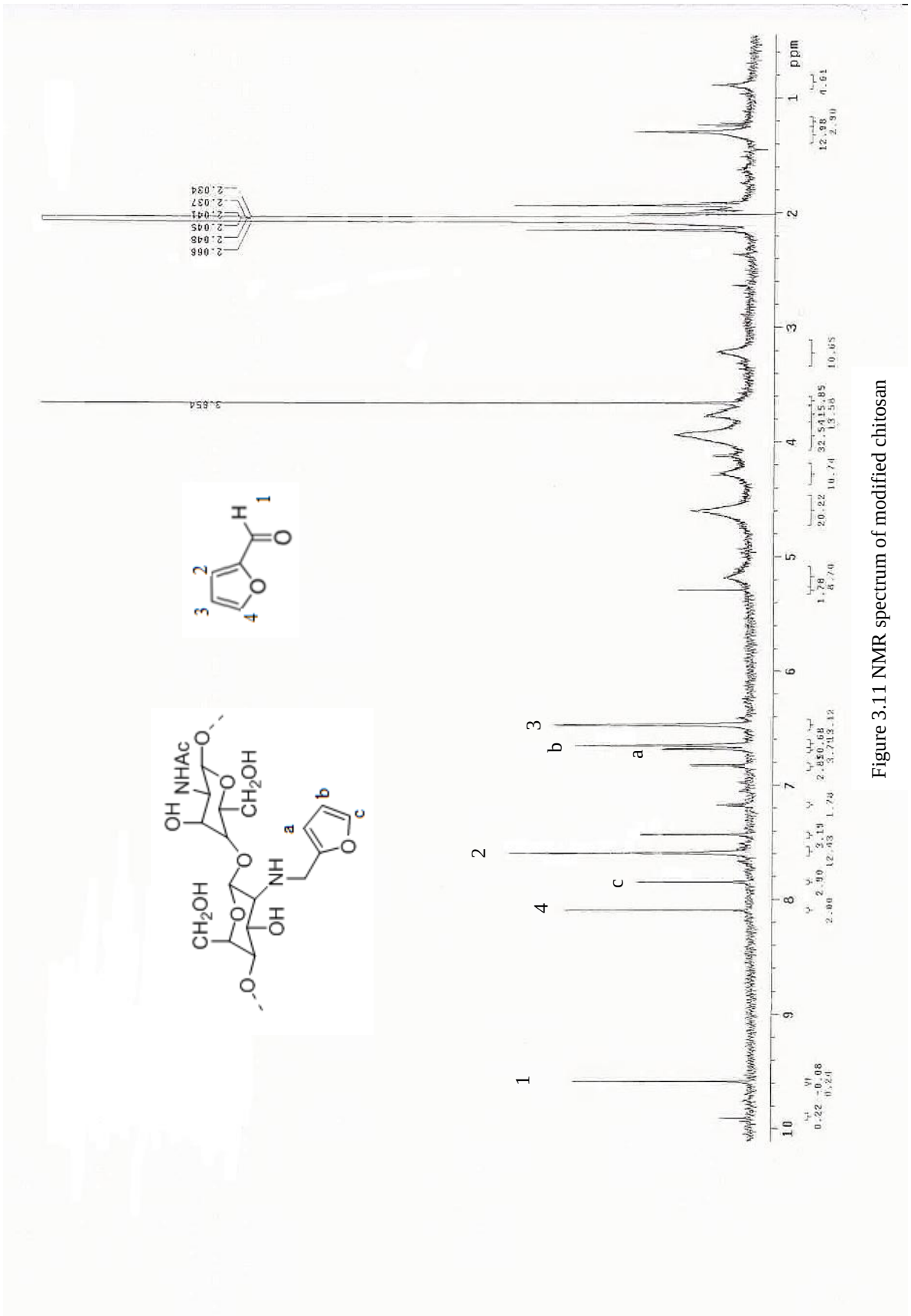

Figure 3.11 NMR spectrum of modified chitosan

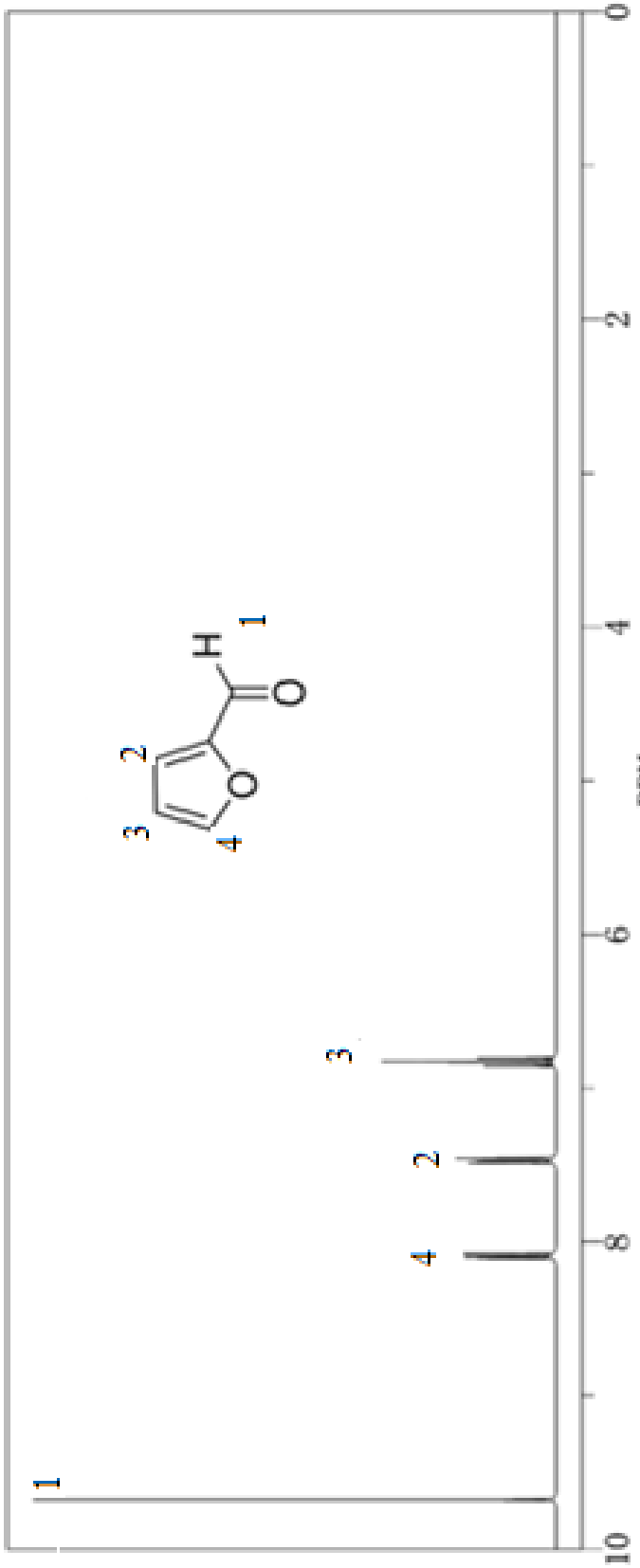

Figure 3.12 NMR spectrum of Furfural

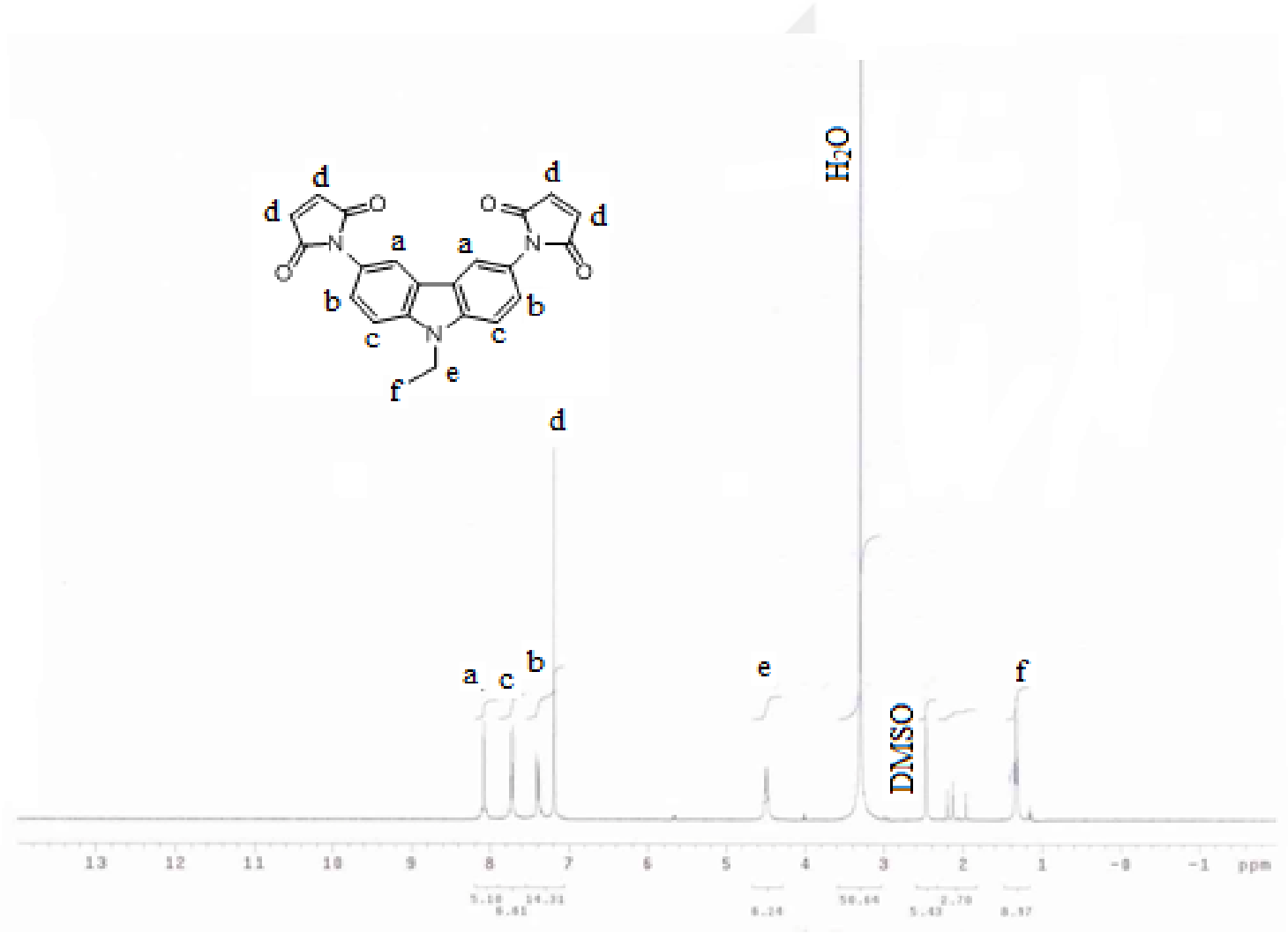

Figure 3.13 NMR spectrum of (1,1'-(9-Etil-9*H*-karbazol-3,6-diil)bis(1*H*-pirol-2,5-dion) (Bismaleimide)

3.2.3 Thermal Analysis

The thermal stability of CF/BMI blend (S) and CF/BMI gels (J) have been investigated by TGA, DTA and DSC under nitrogen flow (Figures 3.14, 3.15, 3.16, 3.17, 3.18). On Table 3.4, the maximum thermal degradation temperatures of dried CF/BMI Gels and their mass losses % were given.

TG/DTA data of the samples were given on Table 3.3 and 3.4. TGA profiles of the samples are presented in Figure 3.14, 3.15. DTA thermograms are presented in Figure 3.16, 3.17. As can be seen from Table 3.3, the maximum degradation temperature of the blend is about 143°C with an average mass loss of 98% and as can be seen from Table 3.4, its gel form has two degredation steps which was highest temperatures about 148°C and 290°C. Furthermore, DTA analyses of the thermograms of the polymers exhibit similar degradation feature except sample MD3S and MD3J.

The DSC curves of dried CF/BMI Gels (J) can be seen from Figure 3.18 as one step of degradation. Table 3.5 shows maximum temperatures of samples. As seen, all samples showed endothermic reactions. MD3J sample demonstrated a minimum temperature as 52°C.

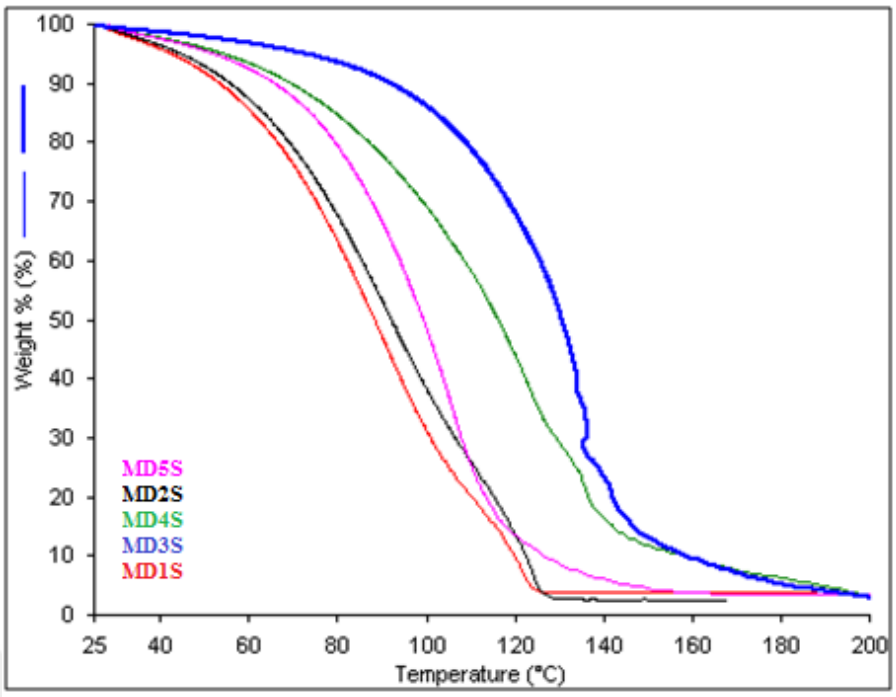

Figure 3.14 TG curves of MD1S, MD2S, MD3S, MD4S and MD5S

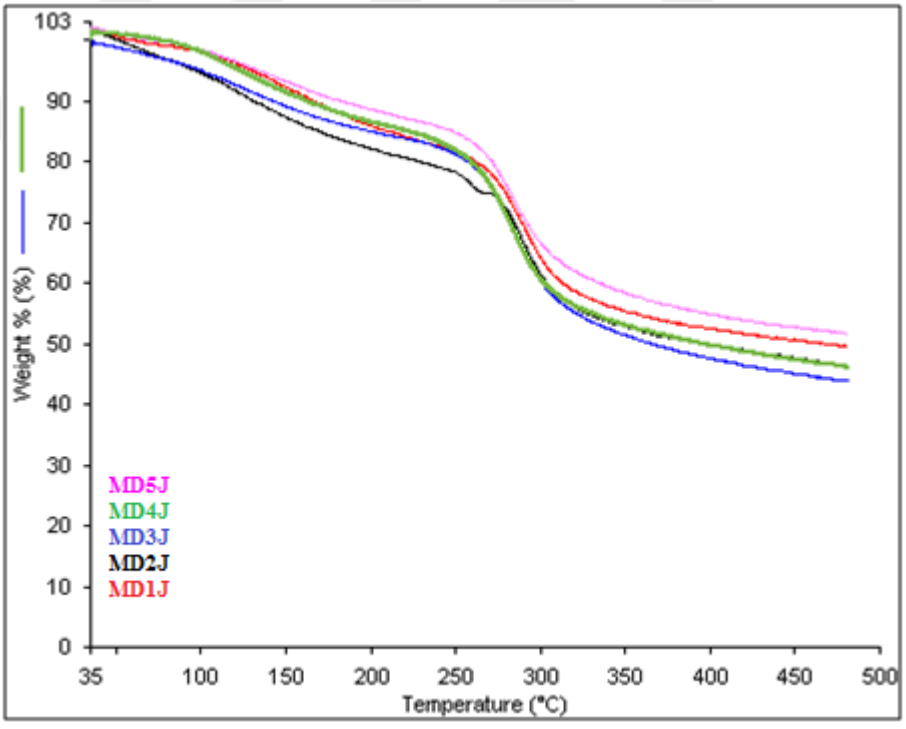

Figure 3.15 TG curves of MD1J, MD2J, MD3J, MD4J and MD5J

Table 3.3 TG data of the blends(S)

Sample	T_{max}/°C	Mass Loss /%
MD1S	116	95
MD2S	120	97
MS3S	143	98
MD4S	141	97
MD5S	116	97

Table 3.4 TG data of the gels(J)

Sample	T_{max}/°C	Mass Loss/%	T_{max}/°C	Mass Loss/%
MD1J	122	20	291	33
MD2J	128	15	285	36
MD3J	148	18	290	34
MD4J	126	15	286	40
MD5J	121	16	283	39

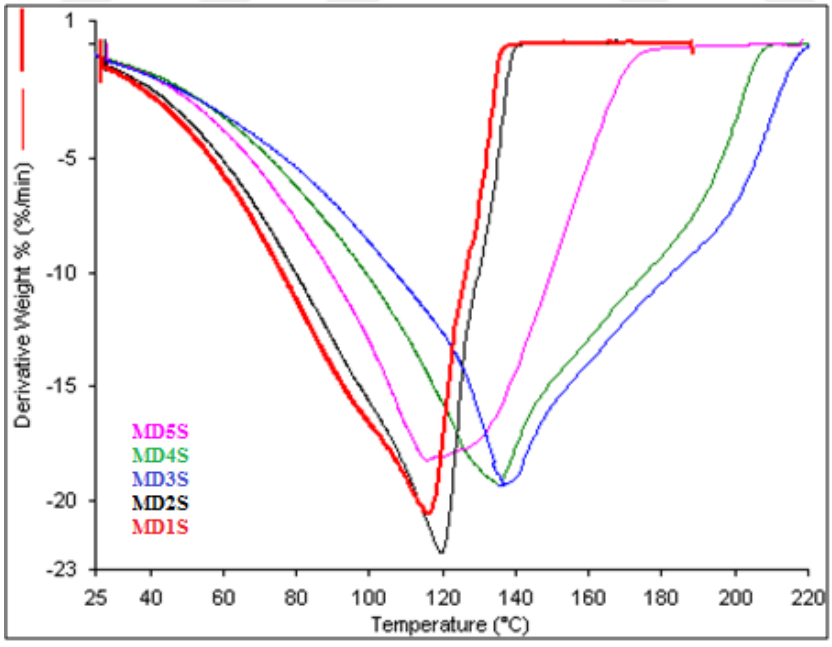

Figure 3.16 DTA curves of MD1S, MD2S, MD3S, MD4S and MD5S

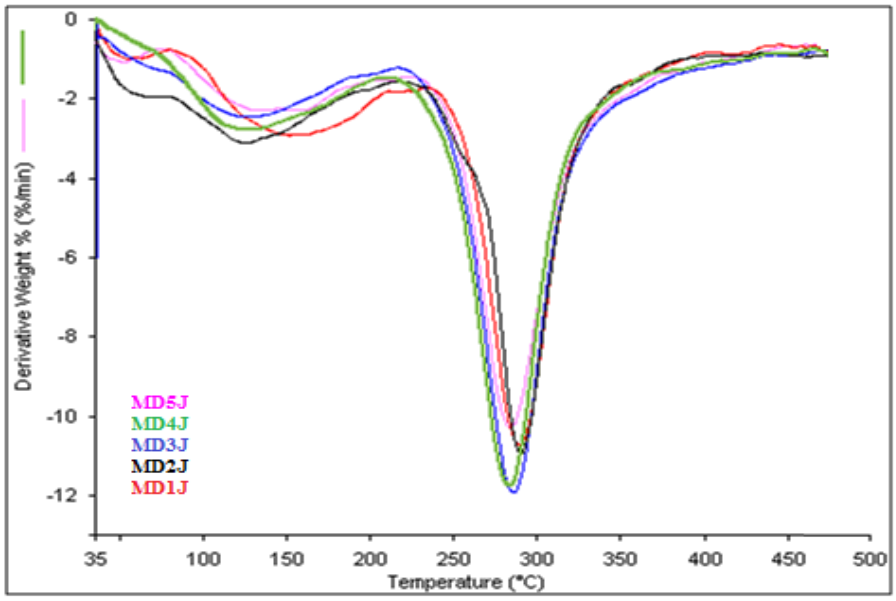

Figure 3.17 DTA curves of MD1J, MD2J, MD3J, MD4J and MD5J

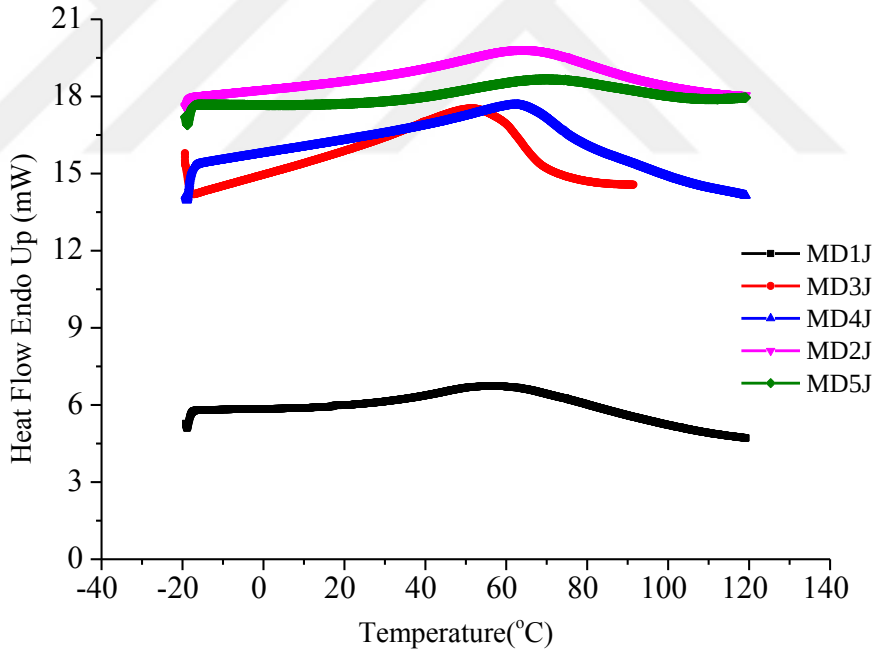

Figure 3.18 DSC curves of MD1J, MD2J, MD3J, MD4J and MD5J in nitrogen flow.

Table 3.5 DSC data of the samples

Sample	T_{max}/°C	Mol Ratio of CF/BMI
MD1J	58	1/100
MD2J	65	1/50
MD3J	52	1/10
MD4J	63	1/5
MD5J	71	1/1

3.2.4 Optical Microscope Analysis

Optical Microscopic analysis of the samples was carried out by using Nikon DS-Fi1 Optical Microscop in Metallurigal and Materials Engineering Department of Engineering Faculty of Dokuz Eylül University.

The coatings on the glass panels were scratched carefully with a bistoury. The self-healing properties of the coated samples were examined after heating at 60 °C for 1 hour with the optical microscope. The images were given in Figure 3.19 -3.24 before heating and after heating at 60°C, respectively.

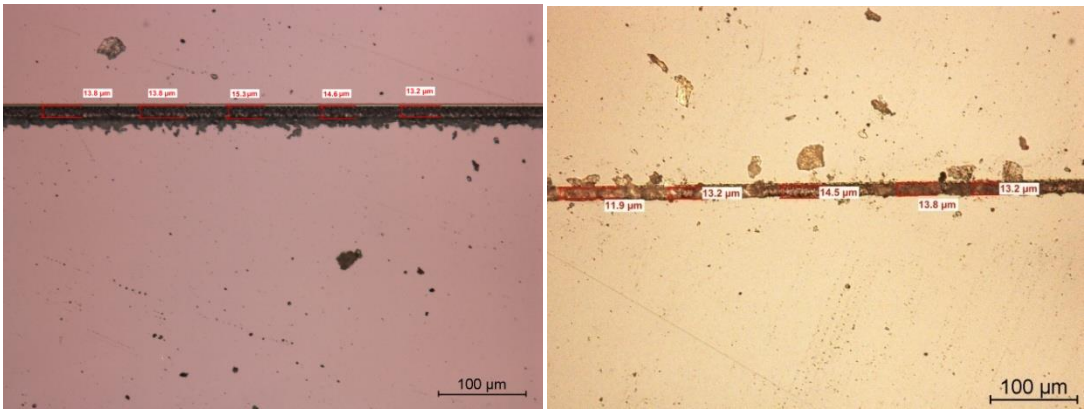

Figure 3.19 Self-healing behavior of Blank sample

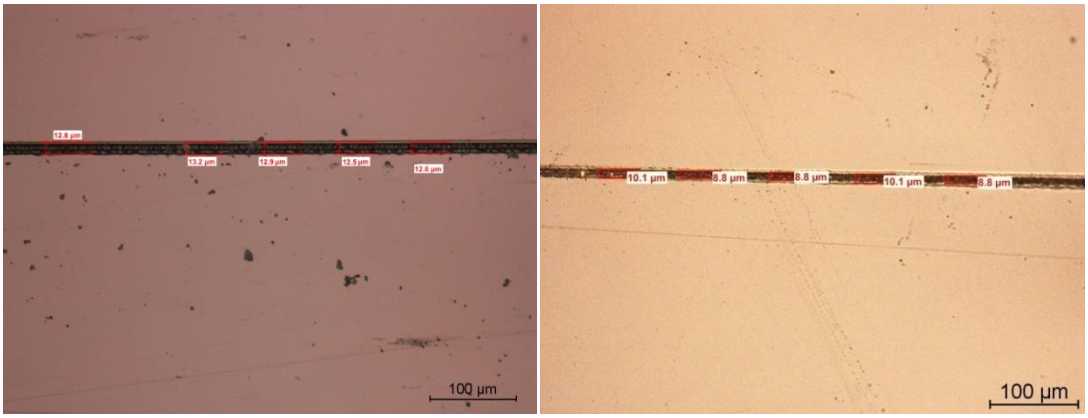

Figure 3.20 Self-healing behavior of MD1V

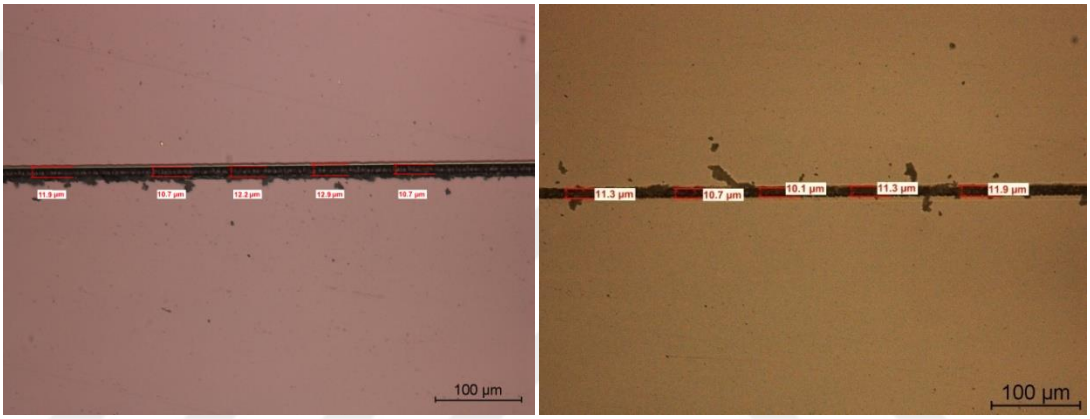

Figure 3.21 Self-healing behavior of MD2V

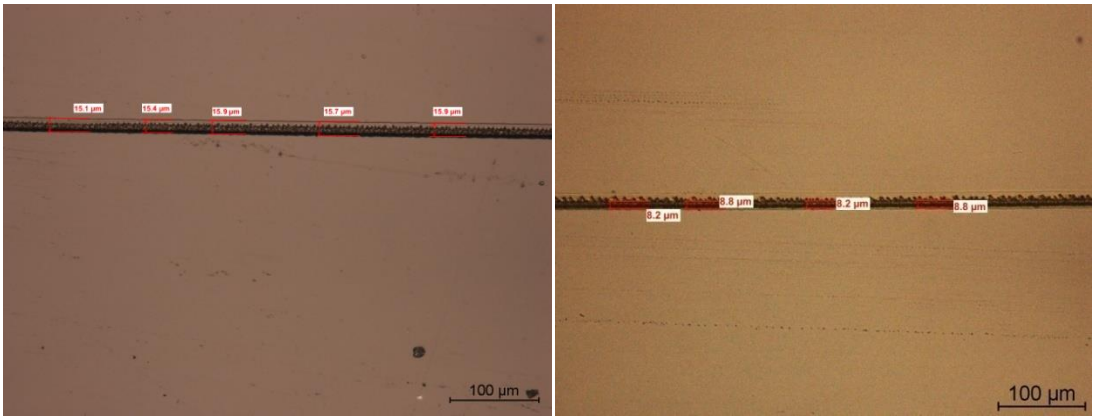

Figure 3.22 Self-healing behavior of MD3V

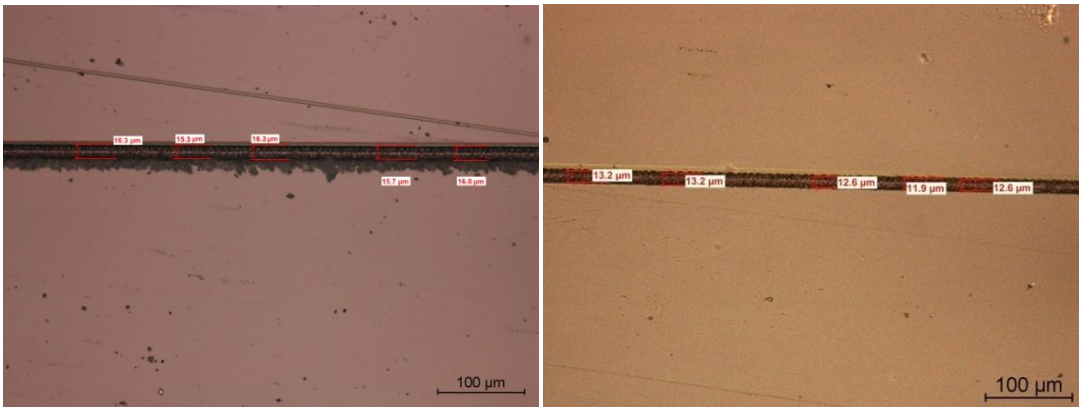

Figure 3.23 Self-healing behavior of MD4V

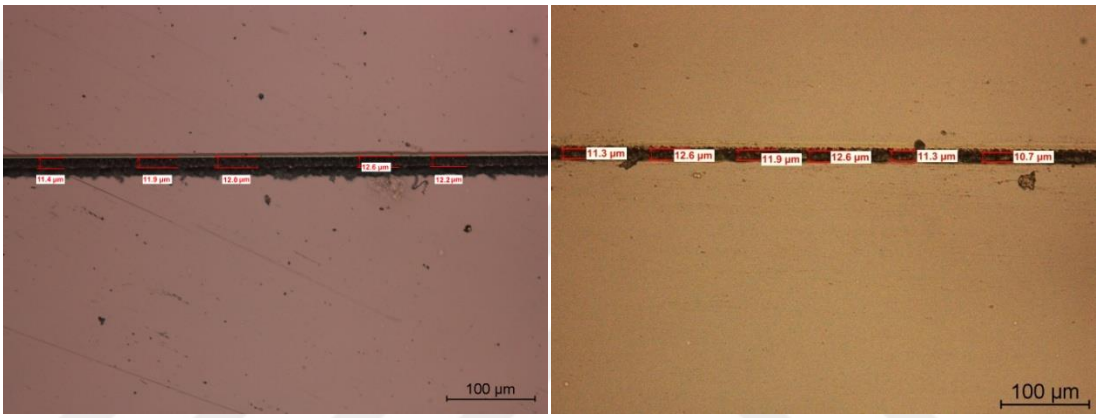

Figure 3.24 Self-healing behavior of MD5V

It has been observed from the above presented OM Images that some healings were observed after heating at 60°C, but not completed at all for all samples. MD1V, MD3V demonstrated the self healing behavior. Before heating at 60 °C the average gap of the line for MD3V is 15.6 µm. After heating at 60 °C, the average gap of the line for MD3V is about 8.5 µm. The similar behavior is seen to for MD1V (12.8 µm to 9.32 µm).

CHAPTER FOUR
CONCLUSIONS

4.1 Capsule-Based Self-Healing

In order to examine the possibility to use the prepared epoxy samples at high temperatures, the samples were cured up to 160 °C. The curing results demonstrated lower healing efficiency which may be due to the catalyst as solid particles embedded in the polymer matrix as in the case of A, B and K samples. The similar results were also observed (Guadagno, Raimondo, Naddeo, & Longo, 2013; Raimondo, Longo, Mariconda, & Guadagno, 2015). In our case, the sample C which was dissolved with MEK had the best self-healing property among the samples as can be seen in Figure 3.5. By using Equation 1, the healing efficiency of the sample C calculated as 80 and 89%. It may be related to solubility of Grubbs' catalyst in the dispersion and its activity. The temperature speeds up the self-healing process in all cases. This study had shown the potential for the development of self-healing property in epoxy type coatings by presenting the healing agents as microcapsules into paints.

4.2 Intrinsic Self-Healing

In the second part of the study, the Diels-Alder Reaction between bismaleimide and chitosan was examined. Poliuretan (PU) acrylic varnish system could show self-healing behaviour due to Diels-Alder reaction between bismaleimide and chitosan-furan which were added in varnish. As it was seen in the DSC analyses, the Diels-Alder reaction temperature was determined as 60°C. The best healing behavior was observed for the samples of MD1V and MD3V. MD1V, MD3V demonstrated the self healing behavior. Before the heating at 60 °C the average gap of the line for MD3V is 15.6 μm. After the heating at 60 °C, the average gap of the line for MD3V is about 8.5 μm. The similar behavior seems to also for MD1V (12.8 μm to 9.32 μm). The healing efficiencies of these samples calculated as 45.5% and 27% respectively. Their mol ratios of CF/BMI were estimated as 1/100 and 1/10

respectively. This study had shown the potential for the development of self-healing property for chitosan and bismaleimide and on this opportunity in acrylic type coatings by presenting the healing agents as Chitosan-Furan and bismaleimide into paints.

As far as healing efficiencies concerned, capsule based self-healing method is better than the intrinsic self-healing. Capsule base self-healing method is more practicle than intrinsic self-healing method due to the fact that modification of chitosan and purity of the samples in which is very important for truly self-healing and also the possible side products reaction of of DA-rDA.

REFERENCES

Arshady, R., & George, M. H. (1993).Suspension, dispersion, and interfacial polycondensation-a methodological survey. *Polymer Engineering and Science, 33,* 865-876.

Asua, J. M. (2002). Miniemulsion polimerization. *Progress in Polymer Science 27,* 1283-1346.

Baycan Koyuncu F., Sefer E., Koyuncu S., & Ozdemir E. (2011). The new branched multielectrochromic materials: Enhancing the electrochromic performance via longer side alkyl chain. *Macromolecules, 44*, 8407-8414.

Baxter, G. (1974). Microencapsulation processes in modern business forms. *In Microencapsulation: Processes and Applications, edited by J. E. Vandegaer (New York: Plenum Press),* 127–143.

Bergman, S. D., & Wudl, F. (2008). Meandable polymers. *Journal of Materials Chemistry, 18,* 41-62.

Bhatia, D., Sarkar, P. C., & Alam, M. (2006).Specular reflectance and derivative spectrometric studies on lac-melamine formaldehyde (MF) resin blends. *Pigment & Resin Technology*, *35*(5), 260-269.

Blaiszik, B. J., Kramer, S. L.B., Olugebefola, S. C., Moore, J. S., Sottos, N.R., & White, S.R. (2010). Self-healing polymers and composites. *Annual Review of Materials Research, 40,* 179-211.

Bleay, S. M., Loader, C. B., Hawyes, V. J., Humberstone, L., & Curtis, P. T. (2001). A smart repair system for polymer matrix composites. *Composites, (A)32,* 1767-1776.

Braun, D., & Legradic, V. (1974). Strukturuntersuchungen an Melamin-Formaldehyd-Reaktionsprodukten. *Makromolecular Materials and Engineering*, *36*, 41-55.

Brown, E. N., Sottos, N. R., & White, S. R. (2002). Fracture testing of a self- healing polymer composite. *Experimental Mechanics, 42(4),* 372-379.

Brown, E. N., White, S. R., & Sottos, N. R. (2004). Microcapsule induced toughening in a self-healing polymer composite. *Journal of Materials Science29,* 1703–1710.

Chen, X. X., Dan, M. A., Ono, K., Mal, A., Shen, H. B., Nutt, S. R., Sheran, K., & Wuld, F. (2002). A thermally remendable cross-linked polymeric material. *Science, 295(5560),* 1698-1702.

Chen, X. X., Wudl, F., Mal, A. K., Shen, H. B., & Nutt, S. R. (2003). New thermally remendable highly cross-linked polymeric materials. *Macromolecules, 36,* 1802-1807.

Cho, S. H., Andersson, H. M., White, S. R., Sottos, N. R., & Braun, P. V. (2006). Polydimethylsiloxane-based self-healing materials. *Advanced Materials, 18,* 997-1000.

Cho, S. H., White, S. R., & Braun, P. V. (2009). Self-healing polymer coatings. *Advanced Materials, 21,* 645-649.

Coma, V. (2013). Polysaccharide-based Biomaterials with Antimicrobial and Antioxidant Properties. *Polímeros, 23(3),* 287-297.

Cordier, P., Tournilhac, F., Soulie-Ziakovic, C., & Leibler, L. (2008). Self-healing and thermoreversible rubber from supramolecular assembly. *Nature 451,* 977-980.

Costa, E. S. C., Jr., & Mansur, H. S. (2007). Preparation and characterization of chitosan/poly(vinyl alcohol) blend chemically cross linked by glutaraldehyde for tissue engineering application. *In Analis of 9 Congresso Brasileiro de Polímeros Campina Grande, PB Brazil, 1,* 86.

Dambies, L., Guimon, C., Yiacoumi, S., & Guibal, E. (2001). Characterization of metal ion interactions with chitosan by X-Ray photoelectron spectroscopy. *Colloids and Surfaces A: Physiochemical and Engineering Aspects, 17,* 203–214.

Dietrich, K., Herma, H., Nastke, R., Bonatz, E., & Teıge, W. (1989). Amino resin microcapsules. *Acta Polymerica, 40,* 243–251.

Dry, C. M., & Sottos, N.R. (1993). Passive smart self-repair in polymer matrix composite materials. *Smart Structures and Materials, 1916,* 438-444.

Dry, C. M. (1996). Procedures developed for self-repair of polymer matrix composite materials. *Composite Structures, 35,* 263-269.

Dunky, M. (1998).Urea-formaldehyde (UF) adhesive resins for wood. *International Journal of Adhesion & Adhesives, 18,* 95-107.

Dutta, P. K., Dutta, J., Chattopadhyaya, M. C., & Tripathi, V. S. (2004). Current aspectson chemical modification of chitosan. *Journal Polymer Materials, 21,* 321–334.

Findon, A., McKay, G., & Blair, H. S. (1993). Transport studies for the sorption of copper ions by chitosan. *Environment Science Health, 28,* 173–185.

Gandini, A. (2005). The application of the diels-alder reaction to polymer syntheses based on furan/maleimide reversible couplings. *Polímeros: Ciência e Tecnologia, 15,* 95-101.

Ghosh, B., & Urban, M. W. (2009). Self-Repairing Oxetane-Substituted Chitosan Polyurethane Networks. *Science, 323,* 1458-1460.

Guadagno, L., Raimondo, M., Naddeo, C., & Longo, P. (2013). Self-healing polymers: from principles to applications, "Application of Self-Healing Materials in Aerospace Engineering". In: Self-healing polymers: from principles to applications. Binder, W.H., editor. *Weinheim: Wiley-VCH Books,* 401-412.

Hansen, C. J., Wu, W., Toohey, K. S., Sottos, N. R., White, S. R., & Lewis, J. A. (2009). Self-healing materials with interpenetrating microvascular networks. *Advanced Materials, 21,* 4143- 4147.

Hayes, S. A., Zhang, W., Branthwaite, M., & Jones, F. R. (2007). Self-healing of damage in fiber-reinforced polymer-matrix composites. *Journal of Royal Society Interface, 4(13),* 381–387.

Hayes, S. A., Jones, F. R., Marshiya, K., & Zhang, W. (2007). A self-healing thermosetting composite material. *Composites A 38(4),* 1116–1120.

Jia Z., Shen, D., & Xu, W. (2001). Synthesis and antibacterial activities of quaternary ammonium salt of chitosan. *Carbohydrate Research, 333,* 1-6.

Craven, J. M, (1969). *US Patent, 3,* 435 003.

Kalista, S. J., Ward, T. C., & Oyetunji, Z. (2007). Self-healing of poly(ethylene-comethacrylic acid) copolymers following projectile puncture. *Mechanics of Advanced Materials and Structures, 14,* 391–397.

Kalista, S., & Ward, T. (2007). Thermal characteristics of the self-healing response in poly(ethylenecomethacrylic acid) copolymers. *Journal of Royal Society Interface, 4,* 405–411.

Keller, M. W., White, S. R., & Sottos, N. R. (2007). A self-healing poly(dimethyl siloxane) elastomer. *Anvanced Functional Materials, 17,* 2399-2404.

Keller, M. W., White, S. R., & Sottos, N. R. (2008). Torsion fatigue response self-healing poly(dimethylsiloxane) elastomers. *Polymer, 49,* 3136-3145.

Kessler, M. R. (2007). Self-healing: a new paradigm on materials design. *Proc. IMechE Vol. 221 Part G: J. Aerospace Engineering, Special Issues Paper, 221,* 479-495.

Kim, C. H., Choi, J. W., Chun, H. J., & Choi, K. S. (1997). Synthesis of chitosan derivatives with quaternary ammonium salt and their antibacterial activity, *Polymer Bulletin, 38,* 387-393.

Koyuncu S., Kaya I., Baycan Koyuncu, F., & Ozdemir, E. (2009). Electrochemical, optical and electrochromic properties of imine polymers containing thiophene and carbazole units. *Synthetic Metals, 159,* 1034-1042.

Kumar, A., Stephenson, L., & Murray, J. (2006). Self-healing coating for steel. *Progress in Organic Coatings, 55,* 244-253.

Kumar, S., & Koh, J. (2012).Physicochemical, optical and biological activity of chitosan–chromone derivative for biomedical applications. *International Journal of Molecular Sciences, 13,* 6102–6116.

Kumar, S., Koh, J., Kim, H., Gupta, M. K., & Dutta, P. K. (2012). A new chitosan-thymine conjugate: Synthesis, characterization and biological activity. *International Journal of Biological Macromolecules, 50,* 493–502.

Kurita, K. (2001). Controlled functionalization of the polysaccharide chitin. *Progress in Polymer Science, 26,* 1921 –1971.

Liu, Y.-L., & Hesieh, C.-Y. (2006). Crosslinked epoxy materials exhibiting thermal remendablility and removability from multifunctional maleimide and furan compounds. *Journal of Polymer Science 44,* 905-913.

Loughran, G. A., Ehlers, G. F. L., Crawford, W.J., Burkett, J. L., & Ray, J. D. (1964). The infrared spectra of some new derivatives of *S*-triazine. *Appied Spectroscopy,18(5),* 129-134.

Luo, X. F., Ou, R. Q., Eberly, D.E., Singhal, A., Viratyaporn, W., & Mather, P. T. (2009). A thermoplastic/thermoset blend exhibiting thermal mending and reversible adhesion. *ACS Applied Materials & Interfaces, 1,* 612–620.

Martin-Matute, B., Nevado, C., Cardenas, DJ., & Echavarren, AM. (2003). Intramolecular reactions of alkynes with furans and electron rich arenes catalyzed by PtCl2: the role of platinum carbenes as intermediates. *Journal of American Chemical Society, 14;125(19),* 5757-5766.

Mathur, N. K., & Narang, C. K. (1990). Chitin and chitosan. versatile polysaccharides from marine animals. *Journal of Chemical Education, 67,* 938.

Montarnal, D., Tournilhac, F., Hidalgo, M., Couturier, J., & Leibler, L. (2009). Versatile one-pot synthesis of supramolecular plastics and self-healing rubbers. *Journal of American Chemical Society, 131,* 7966–7967.

Montiel-Herrera, M., Gandini, A., Goycoolea, F. M., Jacobsen, N. E., Lizardi-Mendoza, J., Recillas-Mota, M., & Ardgüelles-Monal, W. M. (2015). N-(furfural) chitosan hydrogels based on Diels–Alder cycloadditions and application as microspheres for controlled drug release. *Carbohydrate Polymers 128,* 220–227.

Motuku, M., Vaidya, U. K., & Janowski, G. M. (1999). Parametric studies on self-repairing approaches for resin infused composites subjected to low velocity impact. *Smart Materials and Structures, 8,* 623-638.

Muhizi, T., Grelier, S., & Coma, V. (2009) Synthesis of *N*-Alkyl-β-d-glucosylamines and Their Antimicrobial Activity against *Fusarium proliferatum, Salmonella typhimurium, and Listeria innocua. Journal of Agricultural and Food Chemistry, 57,* 11092-11099.

Murphy, E. B., & Wudl F. (2010). The world of smart healable materials. *Progress in Polymer Science, 35,* 223-251.

Padgettll, W. M., Hammer, & W.F. (1958). The Infrared Spectra of Some Derivatives of 1,3,5-Triazine**.** *Journal of the American Chemical Society,80,* 803-808.

Pizzi, A. (1994) *Advanced wood adhesives technology* (2). New York: Marcel Dekker.

Plaisted, T. A., & Nemat- Nasser, S. (2007). Quantitative evaluation of fracture, healing and rehealing of a revesibly cross-linked polymer. *Acta Materialia, 55,* 5684-5696.

Raimondo, M., Longo, P., Mariconda, A., & Guadagno, L. (2015). Healing agent for the activation of self-healing function at low temperature. *Advanced Composite Materials, 24(6),* 519-529.

Renbutsu, E., Hirose, M., Omura, Y., Nakatsubo, F., Okamura, Y., Okamoto, Y., et al. (2005). Preparation and biocompatibility of novel UV-curable chitosan derivatives. *Biomacromolecules, 6,* 2385-2388.

Rinaudo, M. (2006). Chitin and chitosan properties and applications.*Progress in Polymer Science, 31,* 603–632.

Rokhade, A. P., Patil, S. A., & Aminabhavi, T. M (2007). Synthesis and characterization of semi-interpenetrating polymer network microspheres of acrylamide grafted dextran and chitosan for controlled release of acyclovir. *Carbohydrate Polymers, 67,* 605–613.

Sashikala, M., & Ong, H. K. (2007). Synthesis and identification of furfural from rice straw. *Journal of Topic Agriculture and Food Science, 35,* 165-172.

Sashiwa, H. (2005). Chitin and chitosan: novel biomaterials waiting for future developments. *Asian Chitin Journal, 1,* 1–12.

Sugimoto, M., Morimoto, M., Sashiwa, H., Saimoto, H., & Shigemasa, Y. (1998). Preparation and characterization of water-soluble chitin and chitosan derivatives. *Carbohydrate Polymers, 36,* 49–59.

Teramoto, N., Arai, Y., & Shiba, M. (2006). Thermo-reversible diel-alder polymerization of difurfutylidene trehalose and bismaleimides. *Carbohydrate Polymers, 64,* 78-84.

Thies, C. (1987). Microencapsulation. In H. F. Mark, N. Bikales, C. G. Overberger, G. Menges and J. I. Kroschwitz (Ed.). *Encyclopedia of Polymer Science and Engineering* (2nd ed.) (724–745). New York: Wiley.

Thies, C. (1996). A survey of microencapsulation processes. In S. Benita, (Ed.). *Microencapsulation: Methods and Industrial Applications* (1-19). New York: Marcel Dekker Inc.

Trask, R. S., Williams H. R., & Bond, I. P. (2007). Self-healing polymer composites: mimicking nature to enhance performance. *Bioinspiration and Biomimetics, 2,* 1-9.

Ullah, S., Bustam, M. A., Nadeem, M., Naz, M. Y., Tan, W. L., & Shariff, A.M. (2014). Synthesis and thermal degradation studies of melamine formaldehyde resins. *The Scientific World Journal,* Article ID 940502, 6.

Varley, R. J., & van der Zwaag, S. (2008). Towards an understanding of thermally activated self-healing of an ionomer system during ballistic penetration. *Acta Materials, 56,* 5737–5750.

Wan, Y., Creber, K. A. M., Peppley, B., & Bui, V. T. (2004). Ionıc conductivity and tensile properties of hydroxyethyl and hydroxypropyl chitosan membranes. *Journal of Polymer Science Part B Polymer Physics 42,* 1379-1397.

Wang, D., Williams, C. G., Yang, F., & Elisseeff, J. H. (2004a). Enhancing the tissue biomaterial interface: tissue-initiated integration of biomaterials. *Advanced Functional Materials, 14,* 1152–1159.

Wang, H., Hu, S., Cai, S., & Yu, F. (2014). Preparation and properties of bisphenol A epoxy resin microcapsules coated with melamine–formaldehyde resin.*Polymer Bulleti,71*, 2407–2419.

Wang, R., Hu H., He, X., Liu, W., Li, H., Guo, Q., & Yuan, L. (2011). Synthesis and characterization of Chitosan/Urea-Formaldehyde shell microcapsules containing dicyclopentadiene. *Journal of Applied Polymer Science, 121,* 2202-2212.

Wang, T., Turhan, M., & Gunasekaran, S. (2004b). Selected properties of pH sensitive, biodegradable chitosan-poly(vinyl alcohol) hydrogel. *Polymer International, 53,* 911–918.

White, S. R., Sottos, N. R., Geubelle, P. H., Moore, J. S., Kessler, S. R., Sriram, Brown, E. N., & Viswanathan, S. (2001). Autonomic healing of polymer composites. *Nature, 409,* 794-797.

Wool, R.P., & O'Connor, K.M. (1981). A theory of crack healing in polymers. *Journal of Applied Physics 52,* 5953-5963.

Wu, D. Y., Meure, S., & Solomon, D. (2008). Self-healing polymeric materials: A review of recent developments. *Progress in Polymer Science, 33,* 479–522.

Yuan, L., Liang, G.Z., & Xie, J.Q. (2007). Synthesis and characterization of microcapsulated dicyclopentadiene with melamine-formaldehyde resins. *Colloid and Polymer Science, 285*, 781-791.

Zhang, D., Sun, W.-H., Hou, J., Jie, S., & Chang, F. (2006). Polymerization of cyclopentadiene initiated by methylaluminoxane. *Journal of Polymer Science, 44,* 264–272.